*Electronic supplementary information*

# Planar Inorganic Five-Membered Heterocycles with $\sigma+\pi$ Dual Aromaticity in Both $S_0$ and $T_1$ States

Xiaojiao Gu,[a] Le Yang,[a] and Peng Jin*[ab]

[a]School of Materials Science and Engineering, Hebei University of Technology, Tianjin 300130, China

[b]Key Laboratory of Special Functional Materials for Ecological Environment and Information (Hebei University of Technology), Ministry of Education, Tianjin 300130, China

**Table S1** Relative energies (kcal/mol) of the $XY_4$ ring isomers in different spin states at the M06-2X/def2-TZVPPD level of theory.

| | singlet | triplet |
|---|---|---|
| $ON_4$ | 0.0 | 90.9 |
| $OP_4$ | 0.0 | 41.3 |
| $OAs_4$ | 0.0 | 26.2 |
| $OSb_4$ | 0.0 | 9.3 |
| $OBi_4$ | 0.0 | 1.5 |
| $SN_4$ | 0.0 | 90.5 |
| $SP_4$ | 0.0 | 57.3 |
| $SAs_4$ | 0.0 | 28.1 |
| $SSb_4$ | 0.0 | 8.8 |
| $SBi_4$ | 0.0 | 0.4 |

**Table S2** Relative energies (kcal/mol) of the $XY_2Z_2$ ring isomers in different spin states at the M06-2X/def2-TZVPPD level of theory. Please refer to Scheme 1 of main text for the different isomeric forms (I-IV). The lowest-energy ones for each state are highlighted in bold.

| | singlet | | | | triplet | | | |
|---|---|---|---|---|---|---|---|---|
| isomer | I | II | III | IV | I | II | III | IV |
| $ON_2P_2$ | 71.7 | 13.6 | 16.0 | **0.0** | 146.2 | 68.6 | 148.4 | **48.7** |
| $ON_2As_2$ | 56.2 | 10.9 | 19.7 | **0.0** | 130.6 | 34.4 | 68.7 | **22.8** |
| $ON_2Sb_2$ | 64.0 | 11.9 | 31.0 | **4.2** | 156.5 | 148.5 | 48.8 | **0.0** |
| $ON_2Bi_2$ | 65.6 | **0.0** | 45.1 | 12.0 | 143.6 | **7.2** | 62.0 | 17.6 |
| $OP_2As_2$ | **0.0** | 3.7 | 5.9 | 12.7 | **37.7** | 56.6 | 59.1 | 62.0 |
| $OP_2Sb_2$ | 8.4 | **0.0** | 8.4 | 10.9 | 42.1 | **12.8** | 37.5 | 20.0 |
| $OP_2Bi_2$ | 9.9 | **0.0** | 13.0 | 21.2 | 41.2 | **5.5** | 26.1 | 179.1 |
| $OAs_2Sb_2$ | 10.1 | 3.0 | 4.3 | **0.0** | 55.9 | **14.2** | 17.6 | 34.6 |
| $OAs_2Bi_2$ | 6.1 | **0.0** | 3.6 | 6.1 | 119.0 | **4.4** | 15.3 | 157.6 |
| $OSb_2Bi_2$ | **0.1** | 3.5 | 3.6 | 7.7 | 8.2 | 197.6 | **0.0** | 214.1 |
| $SN_2P_2$ | 17.9 | 27.7 | **0.0** | 17.9 | 84.0 | **37.7** | 53.5 | 63.2 |
| $SN_2As_2$ | 0.7 | 4.7 | **0.0** | 5.7 | 70.8 | 52.2 | 40.0 | **30.1** |
| $SN_2Sb_2$ | **0.0** | 11.5 | 10.1 | 8.0 | 19.9 | 556.8 | 241.6 | **8.2** |
| $SN_2Bi_2$ | 39.6 | **12.1**[a] | 62.8 | 45.6[a] | 50.2 | **0.0**[a] | 96.1 | 14.7[a] |
| $SP_2As_2$ | 0.5 | **0.0** | 1.9 | 2.1 | 57.4 | 51.2 | **36.5** | 51.3 |
| $SP_2Sb_2$ | 6.2 | **0.0** | 5.5 | 2.2 | 48.8 | **14.9** | 35.3 | 33.9 |
| $SP_2Bi_2$ | 8.4 | **0.0** | 8.7 | 4.6 | 58.6 | 7.7 | 55.5 | **6.9** |
| $SAs_2Sb_2$ | 5.5 | 2.2 | 2.4 | **0.0** | 51.8 | 40.2 | 61.2 | **33.4** |
| $SAs_2Bi_2$ | 5.3 | 1.2 | 2.5 | **0.0** | 146.6 | 47.8 | 131.1 | **4.7** |
| $SSb_2Bi_2$ | 5.3 | 5.2 | 5.1 | **5.0** | 43.5 | 13.4 | **0.0** | 7.9 |

[a]ring broken after optimization.

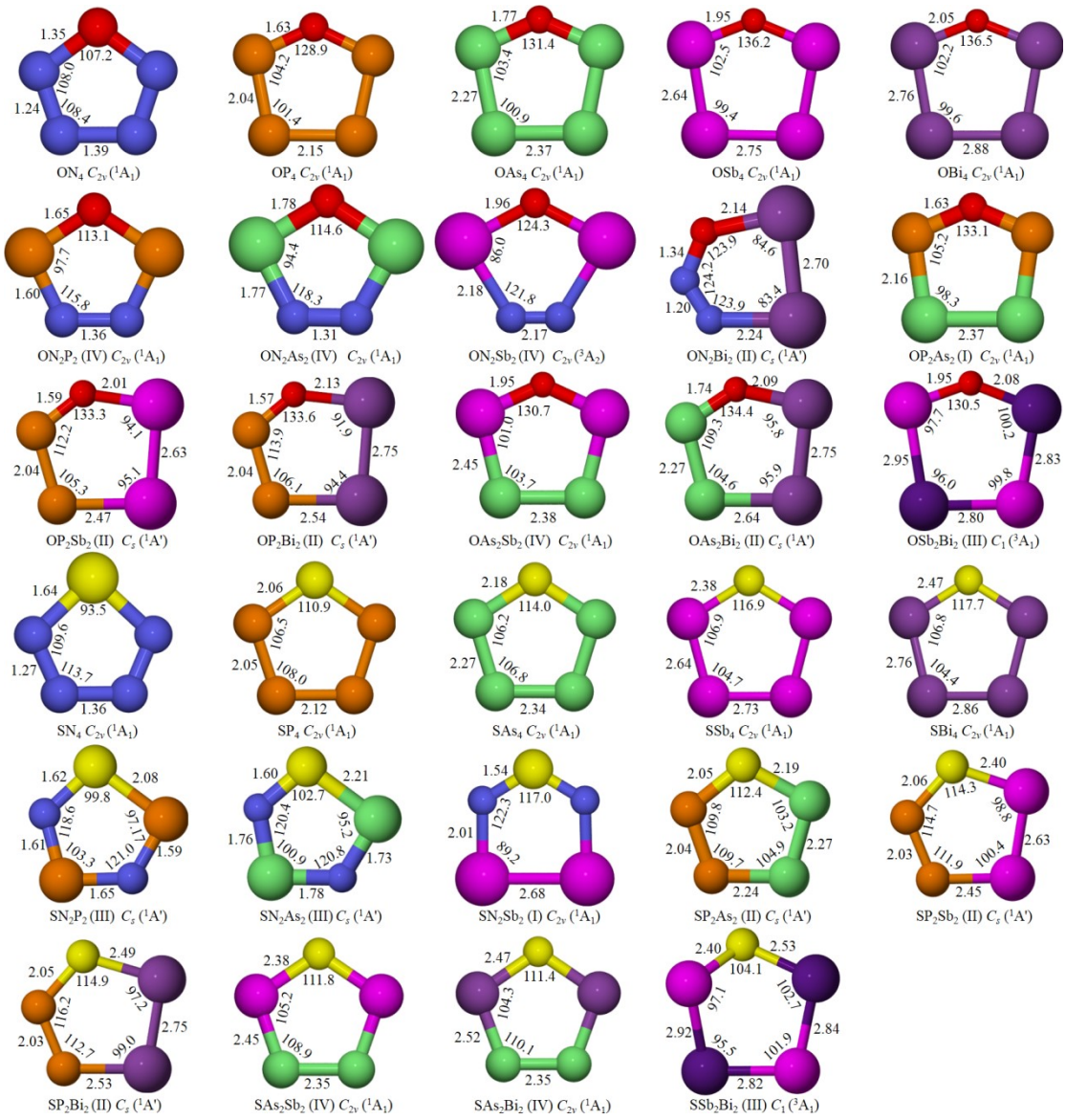


**Fig. S1** Optimized structures and symmetries of the lowest-energy $XY_4$ and $XY_2Z_2$ ring isomers ($S_0$ or $T_0$) in Tables S1 and S2 with bond lengths (in Å) and bond angles (in degree). O: red; S: yellow; N: blue; P: orange; As: green; Sb: bright purple; Bi: dark purple.

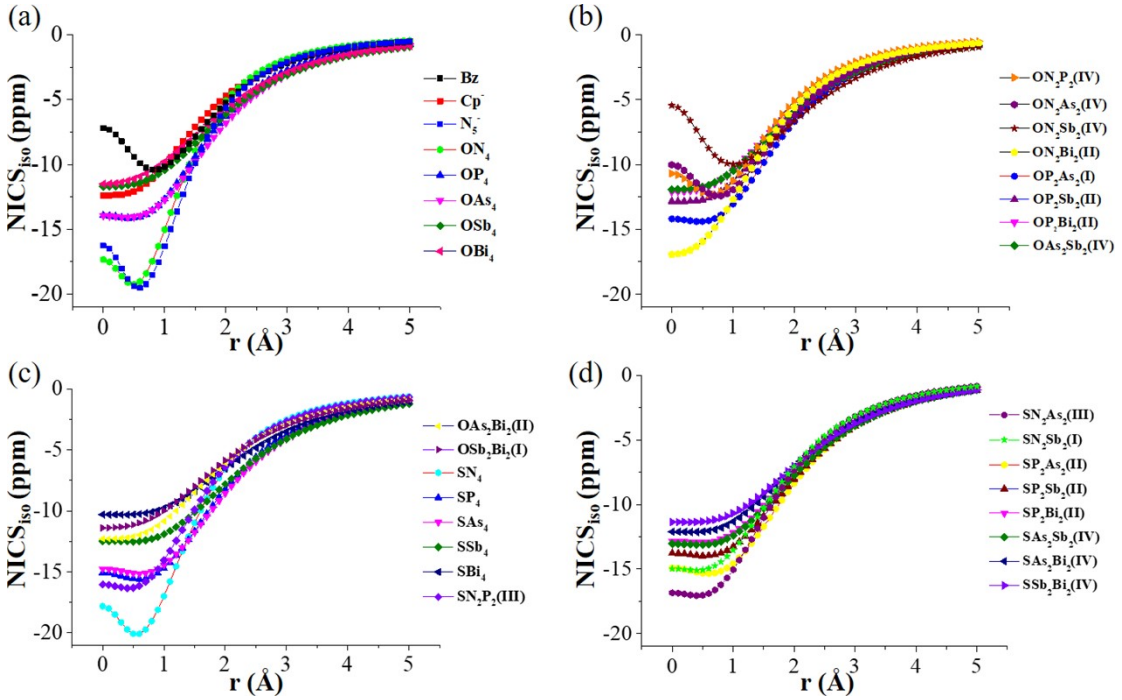


**Fig. S2** (a)-(d) NICS$_{iso}$ profiles along the direction perpendicular to the ring plane of the lowest-lying *singlet* state isomers in Tables S1 and S2 (ring center as the origin).

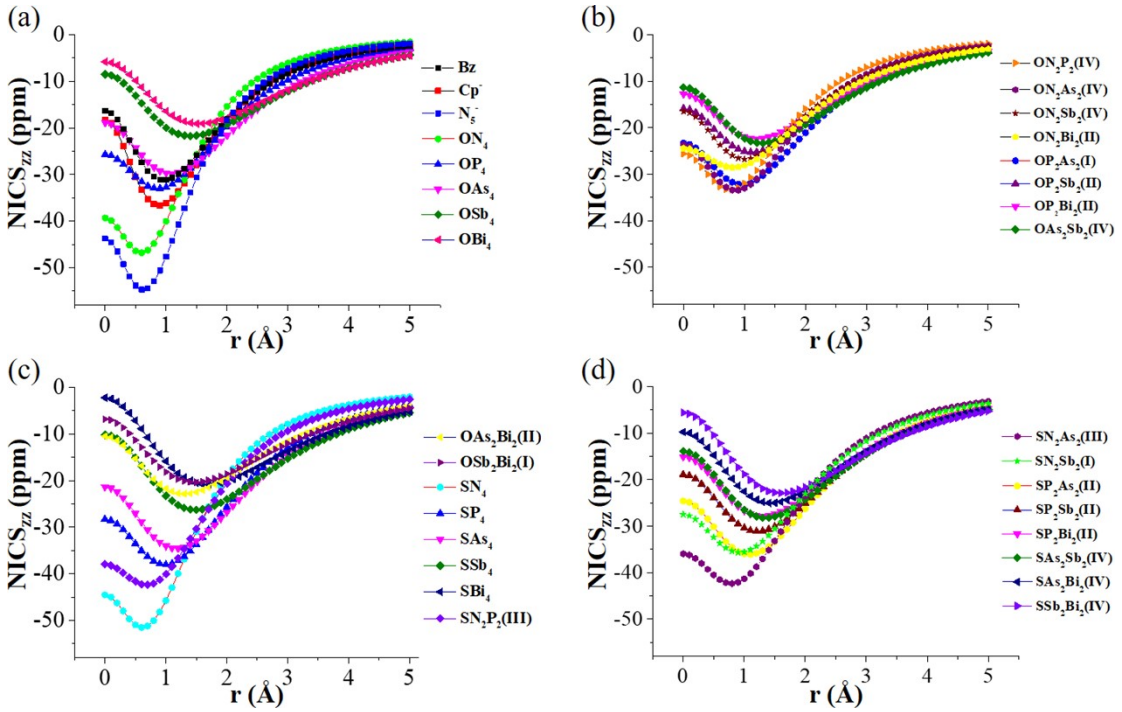


**Fig. S3** (a)-(d) NICS$_{zz}$ profiles along the direction perpendicular to the ring plane of the lowest-lying *singlet* state isomers in Tables S1 and S2 (ring center as the origin).

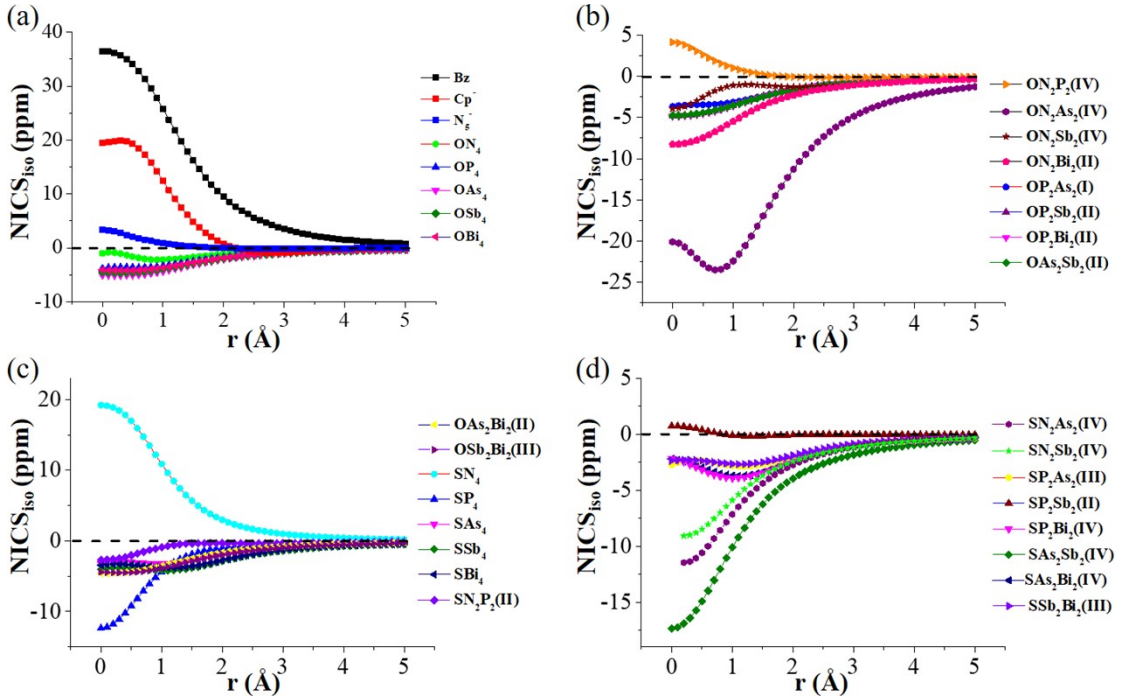


**Fig. S4** (a)-(d) NICS$_{iso}$ profiles along the direction perpendicular to the ring plane of the lowest-lying *triplet* state isomers in Tables S1 and S2 (ring center as the origin).

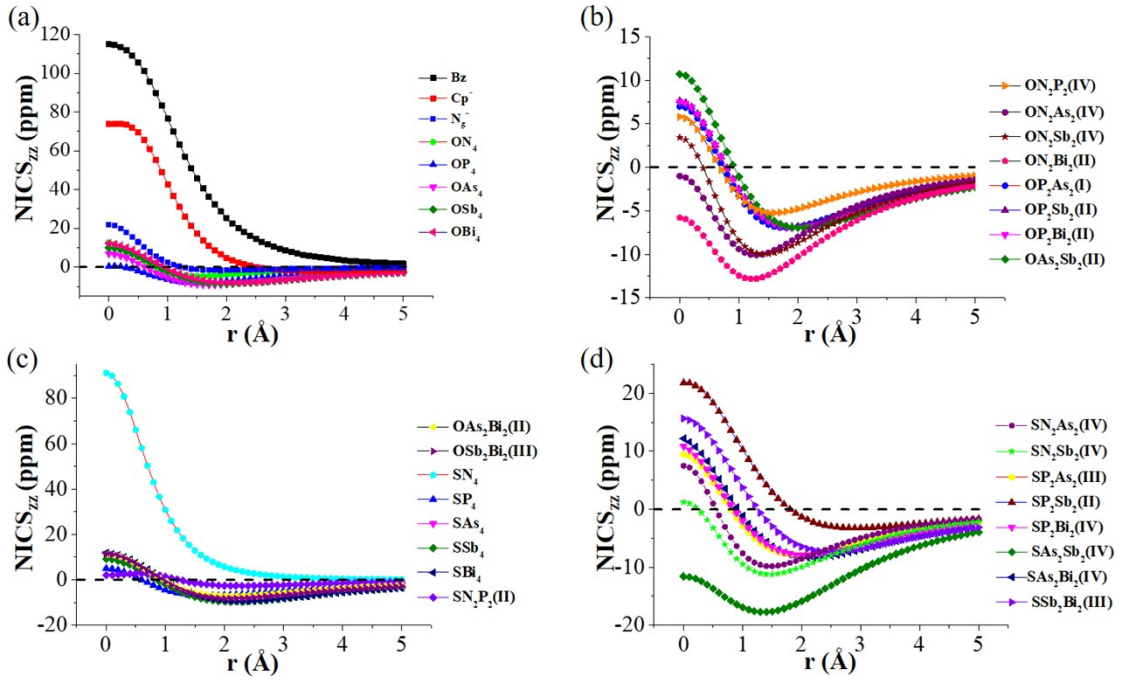


**Fig. S5** (a)-(d) NICS$_{zz}$ profiles along the direction perpendicular to the ring plane of the lowest-lying *triplet* state isomers in Tables S1 and S2 (ring center as the origin).

**Table S3** Formation energy ($E_f$, kcal/mol) and HOMO-LUMO gap energies (eV) of $ON_2As_2$, $ON_2Bi_2$ and $SAs_2Sb_2$ obtained at the M06-2X/def2-TZVPPD level of theory.

| | $S_0$ | | $T_1$ | | |
|---|---|---|---|---|---|
| | $E_f$ | gap | $E_f$ | gap (α) | gap (β) |
| $ON_2As_2$ | 428.3 | 5.34 | 405.5 | 5.52 | 3.75 |
| $ON_2Bi_2$ | 341.7 | 4.84 | 334.5 | 5.33 | 3.80 |
| $SAs_2Sb_2$ | 266.6 | 4.50 | 233.2 | 4.03 | 2.15 |

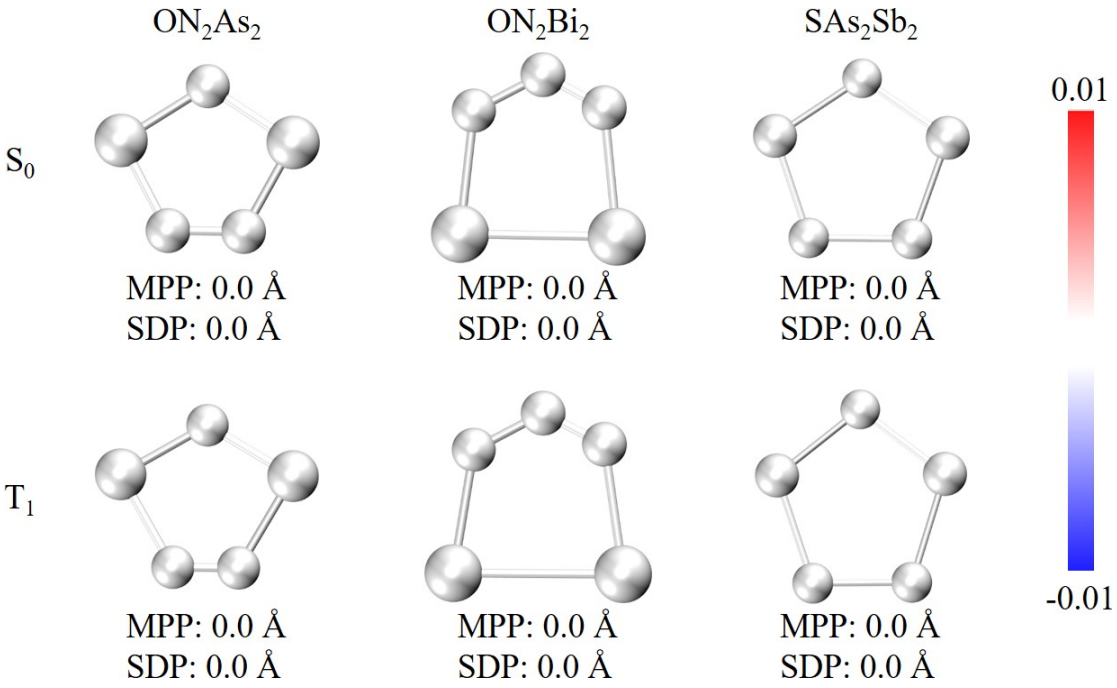


**Fig. S6** Calculated molecular planarity parameter (MPP) and span of deviation from plane (SDP) for the $ON_2As_2$, $ON_2Bi_2$ and $SAs_2Sb_2$ in two electronic states.

As documented in the Multiwfn program manual (Verson 3.8 (dev), 2022-Jul-23) and Ref. S1, the author proposed two rigorous metrics of planarity of a molecule: molecular planarity parameter (MPP) and span of deviation from plane (SDP). For a given set of atoms ($N_{atom}$ atoms), MPP is defined as

$$\mathrm{MPP} = \sqrt{\frac{\sum_i di^2}{N_{atom}}}$$

where $d_i$ is the distance between atom $i$ and the plane fitted for the considered atoms. SDP is defined as $d_{max} - d_{min}$, where $d_{max}$ and $d_{min}$ denote the most positive and most negative $d_i$ for all considered atoms, respectively. MPP can measure the overall degree of deviation of the atoms from the fitting plane, and SDP exhibits deviation span of the system with respect to the fitting plane. Their zero values thus indicate perfect planarity of the studied system.

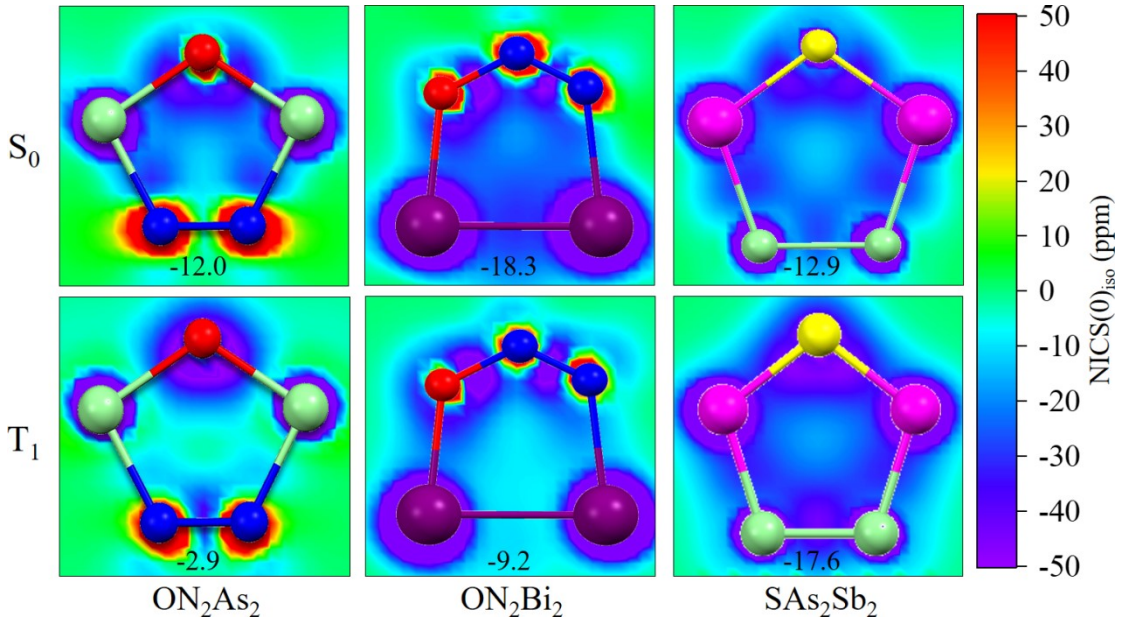


**Fig. S7** Similar NICS(0) grids as Fig. 6 in main text but obtained at the B3LYP/def2-TZVP level of theory (geometry optimization was done at the same level).

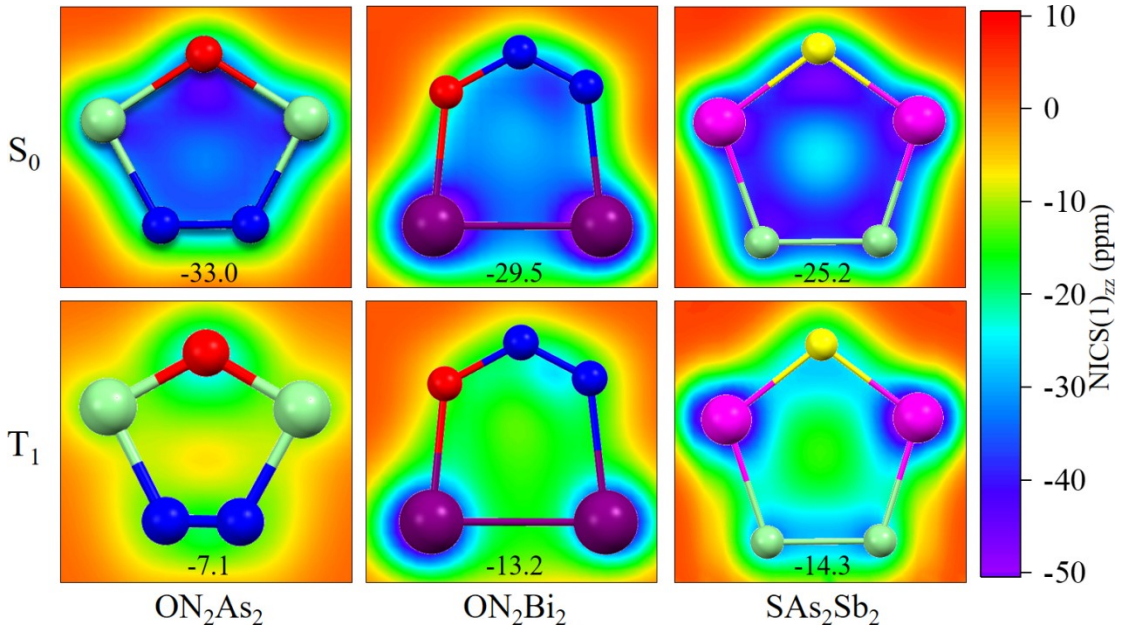


**Fig. S8** Similar NICS(1)$_{zz}$ grids as Fig. 7 in main text but obtained at the B3LYP/def2-TZVP level of theory (geometry optimization was done at the same level).

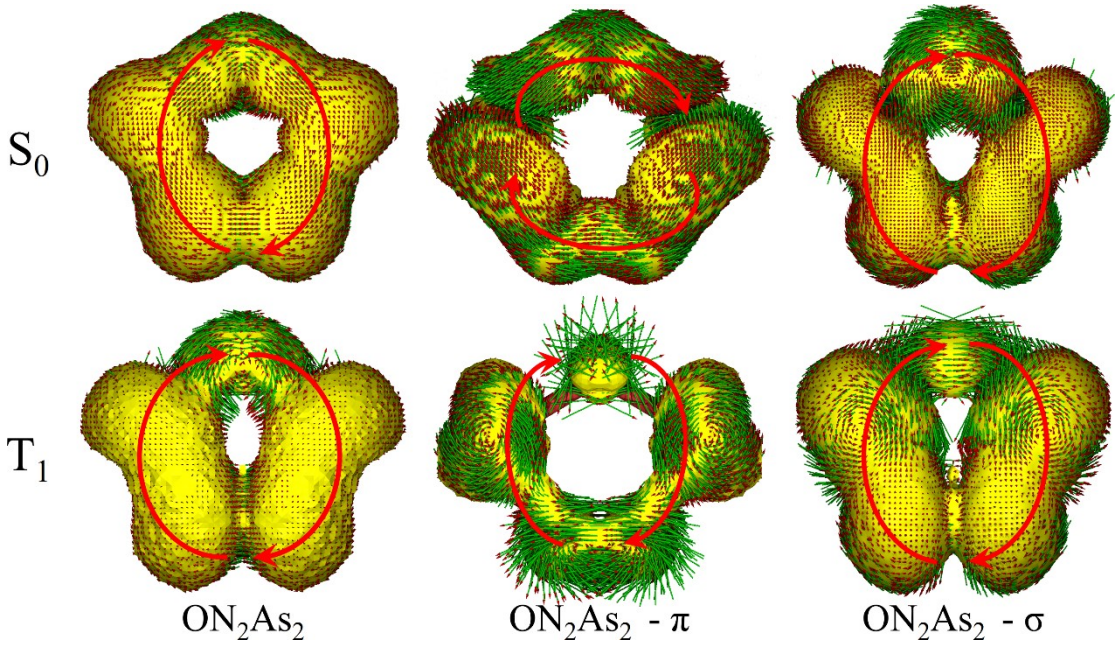


**Fig. S9** ACID isosurfaces (isovalue: 0.024 a.u.) of the $ON_2As_2$ ring in the $S_0$ and $T_1$ states (total, $\pi$ and $\sigma$ contributions). The magnetic field vector is perpendicular to the ring plane and points upward, and clockwise currents thus mean diatropic. Small green arrows denote current density vectors.

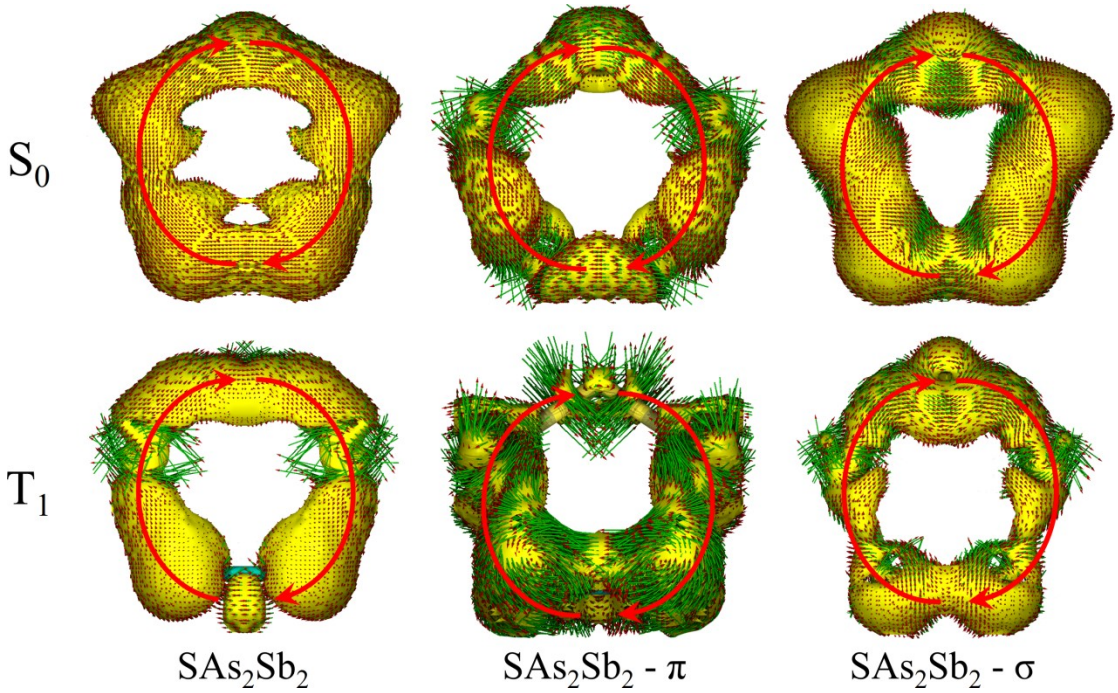


**Fig. S10** ACID isosurfaces (isovalue: 0.024 a.u.) of the $SAs_2Sb_2$ ring in the $S_0$ and $T_1$ states (total, $\pi$ and $\sigma$ contributions). The magnetic field vector is perpendicular to the ring plane and points upward, and clockwise currents thus mean diatropic. Small green arrows denote current density vectors.

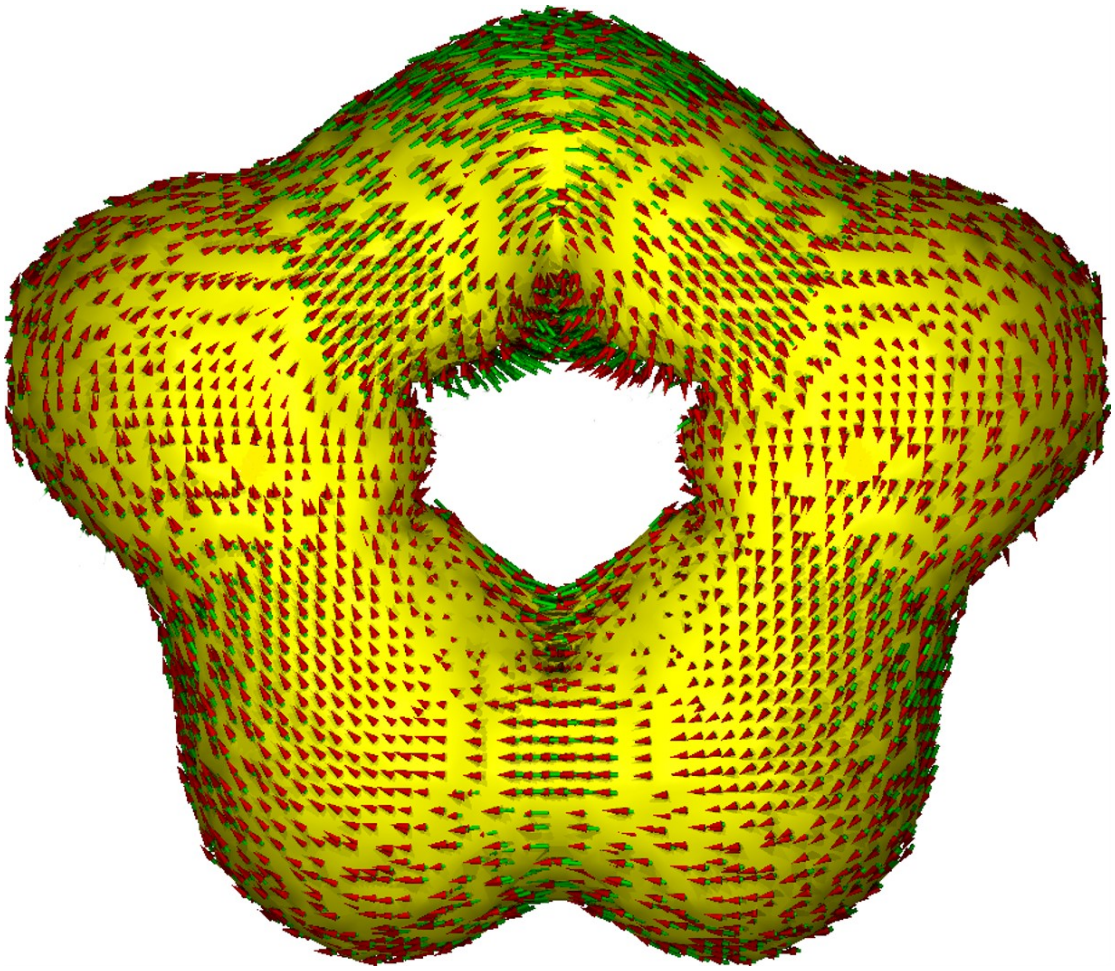

**Fig. S11** ACID isosurface (isovalue: 0.024 a.u.) of the $ON_2As_2$ ring in the $S_0$ state (total).

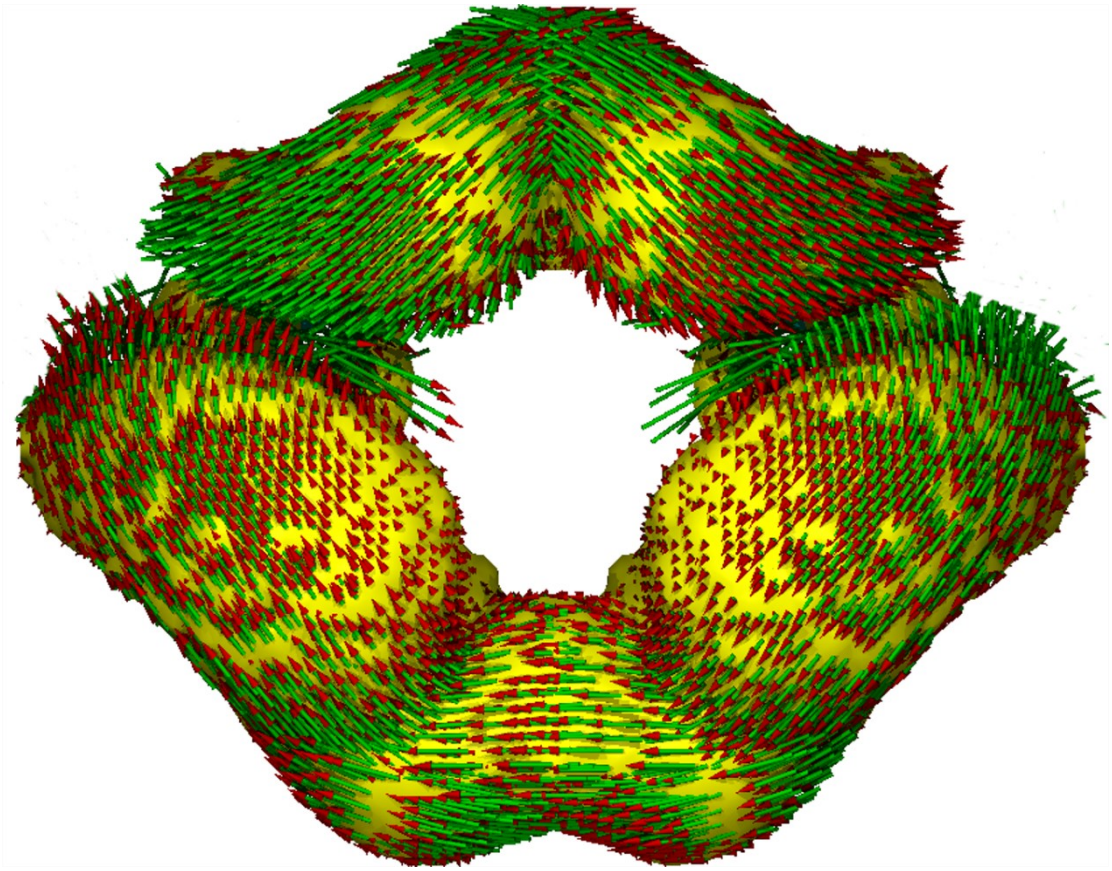

**Fig. S12** ACID isosurface (isovalue: 0.024 a.u.) of the $ON_2As_2$ ring in the $S_0$ state ($\pi$).

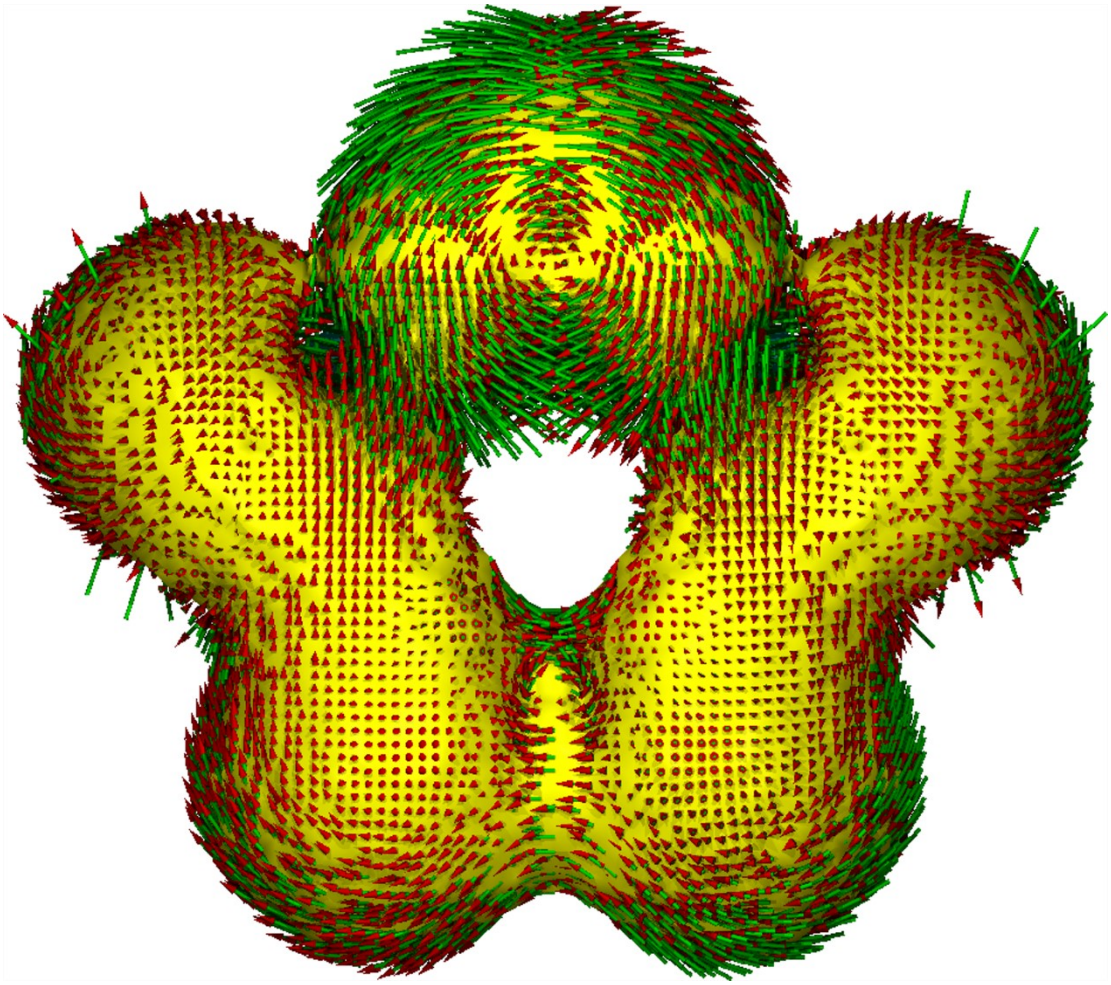

**Fig. S13** ACID isosurface (isovalue: 0.024 a.u.) of the $ON_2As_2$ ring in the $S_0$ state ($\sigma$).

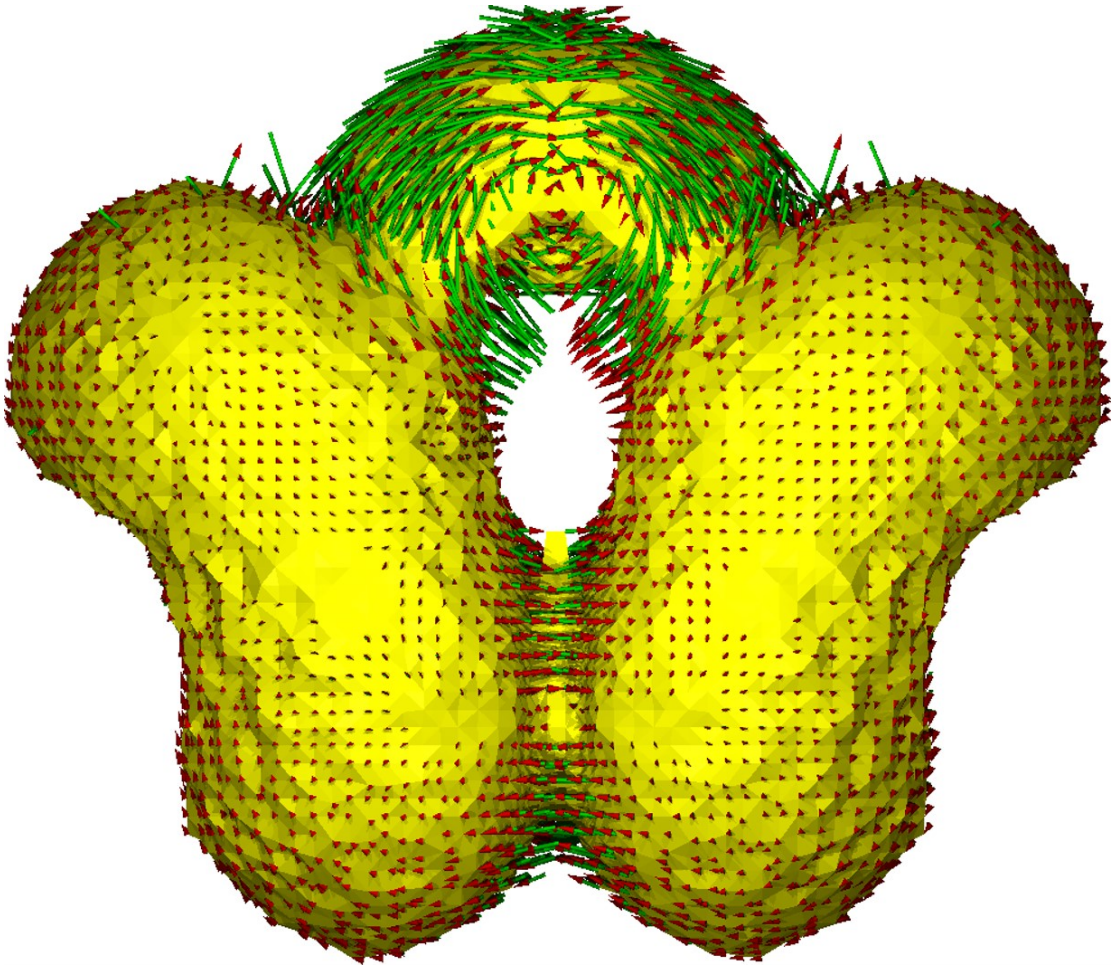

**Fig. S14** ACID isosurface (isovalue: 0.024 a.u.) of the $ON_2As_2$ ring in the $T_1$ state (total).

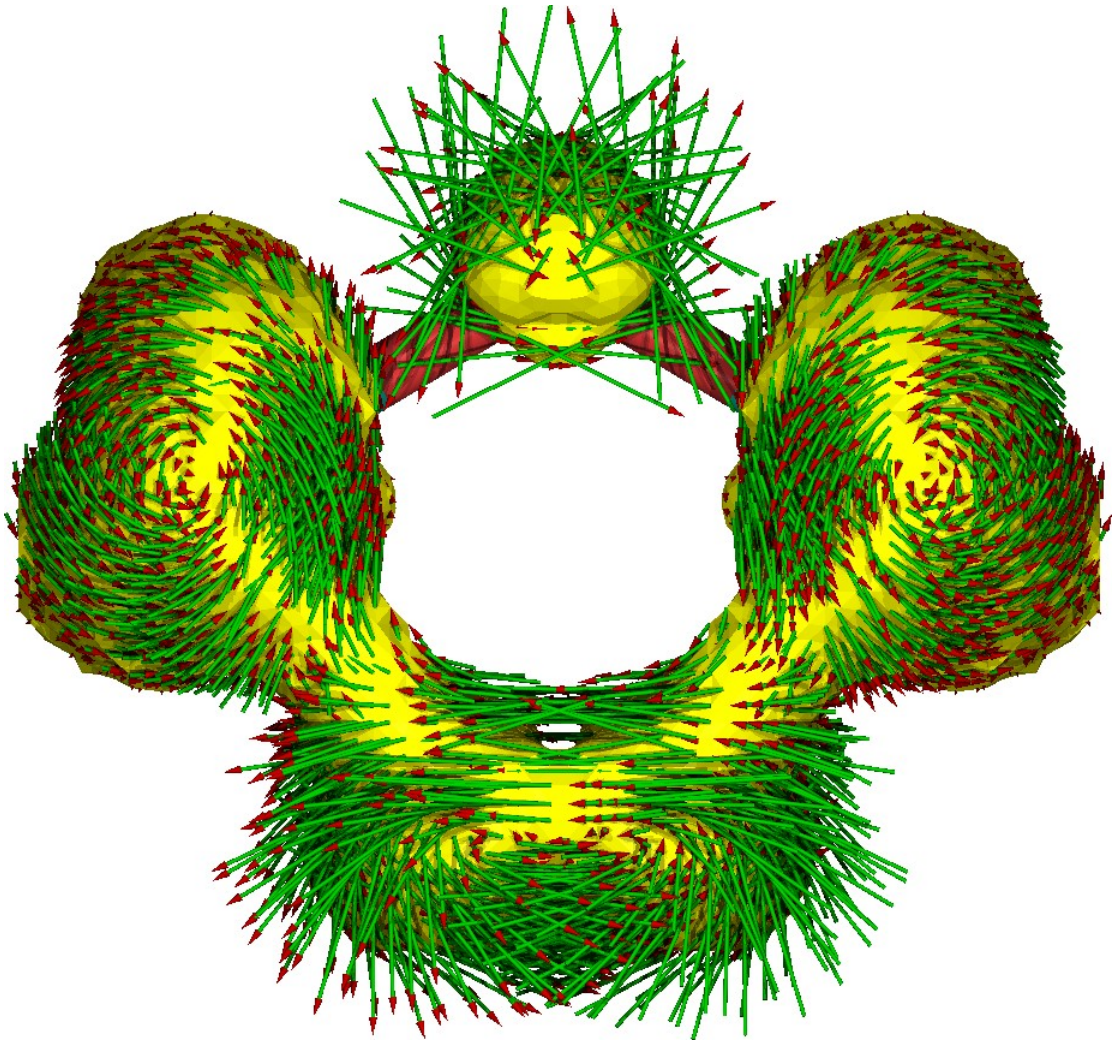

**Fig. S15** ACID isosurface (isovalue: 0.024 a.u.) of the $ON_2As_2$ ring in the $T_1$ state ($\pi$).

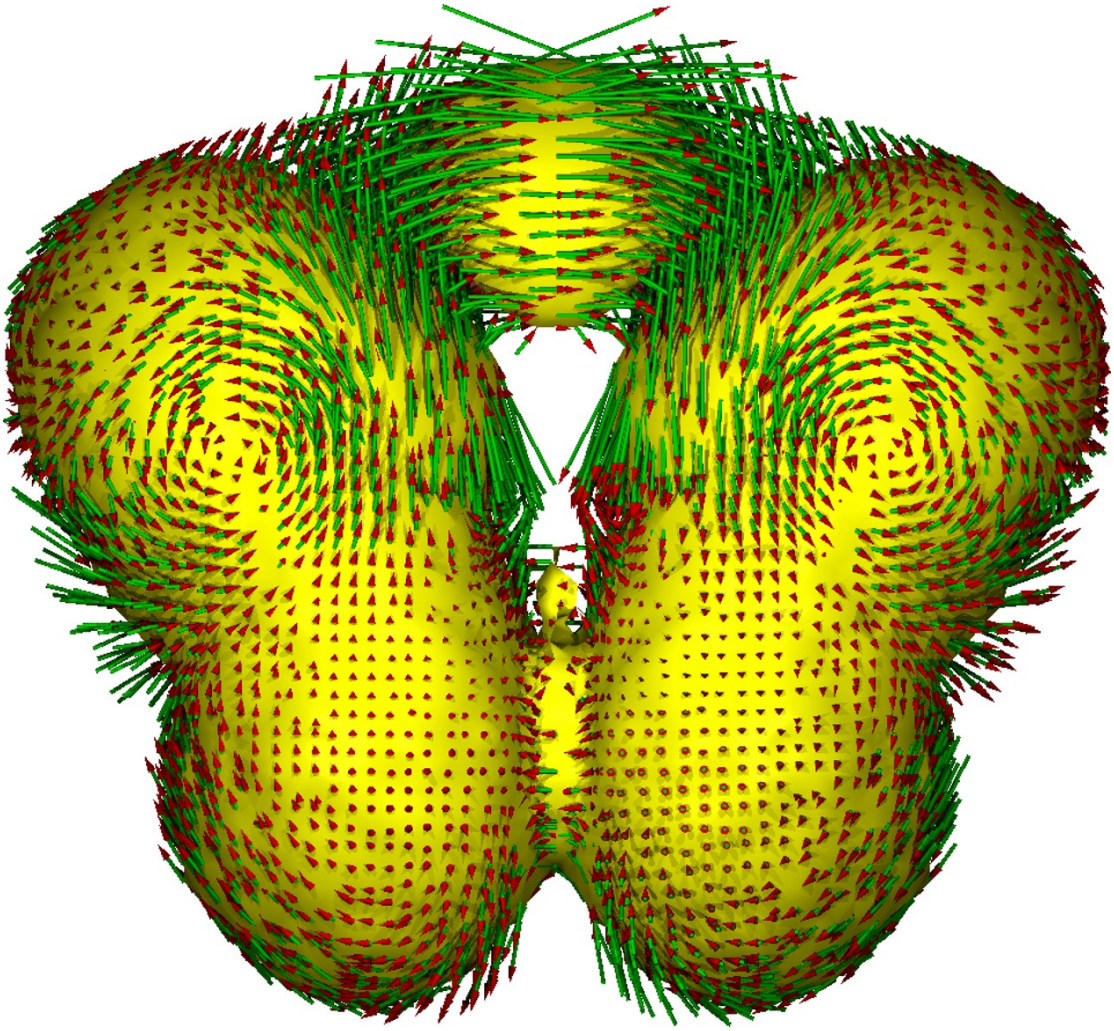

**Fig. S16** ACID isosurface (isovalue: 0.024 a.u.) of the $ON_2As_2$ ring in the $T_1$ state ($\sigma$).

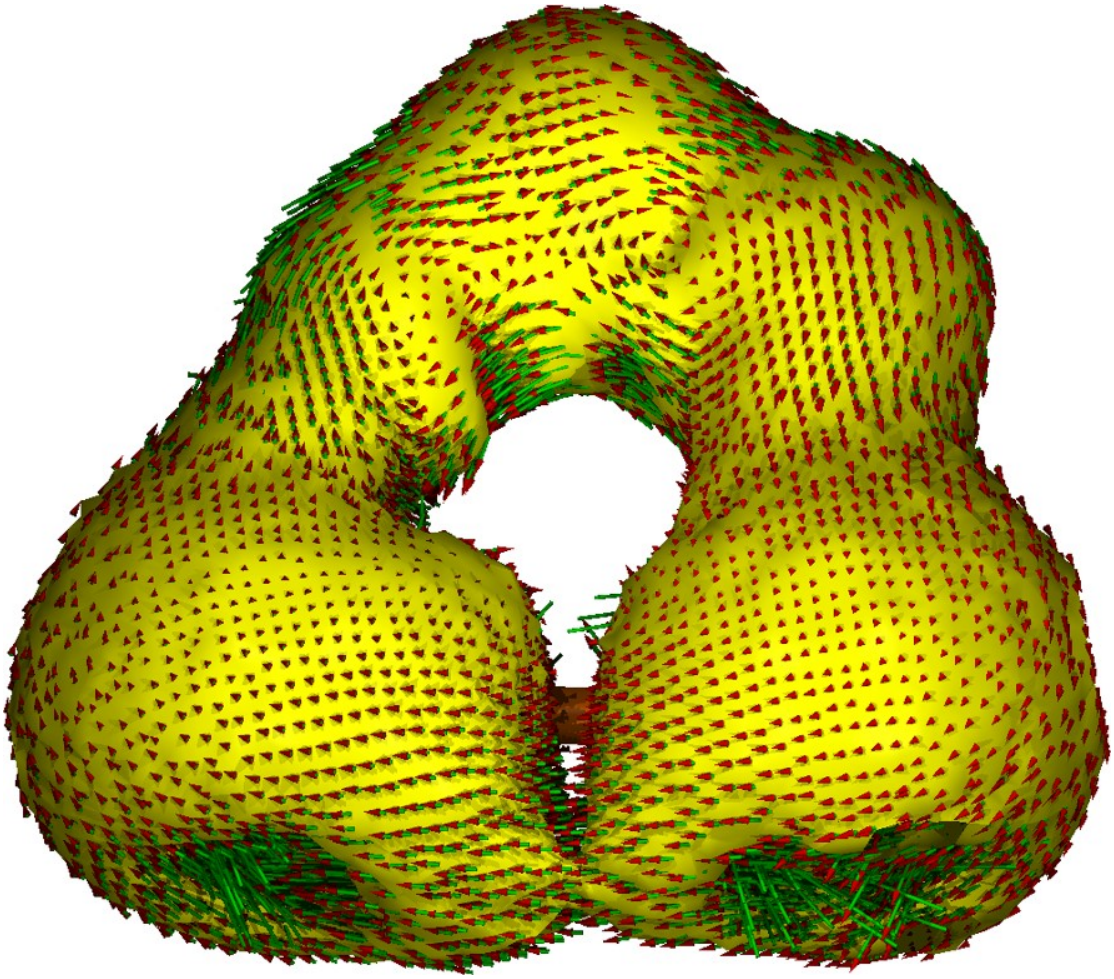

**Fig. S17** ACID isosurface (isovalue: 0.024 a.u.) of the $ON_2Bi_2$ ring in the $S_0$ state (total).

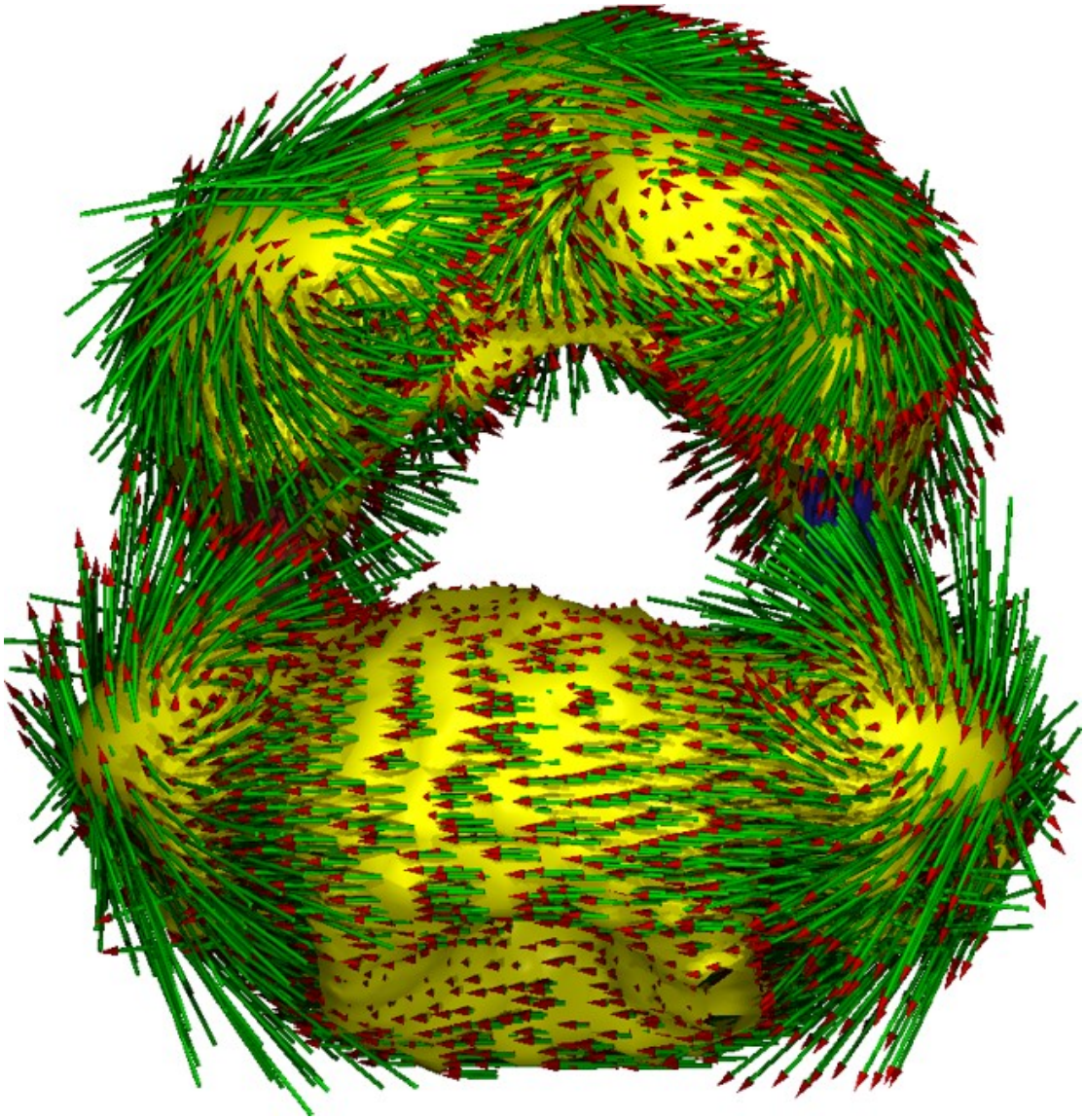

**Fig. S18** ACID isosurface (isovalue: 0.024 a.u.) of the $ON_2Bi_2$ ring in the $S_0$ state ($\pi$).

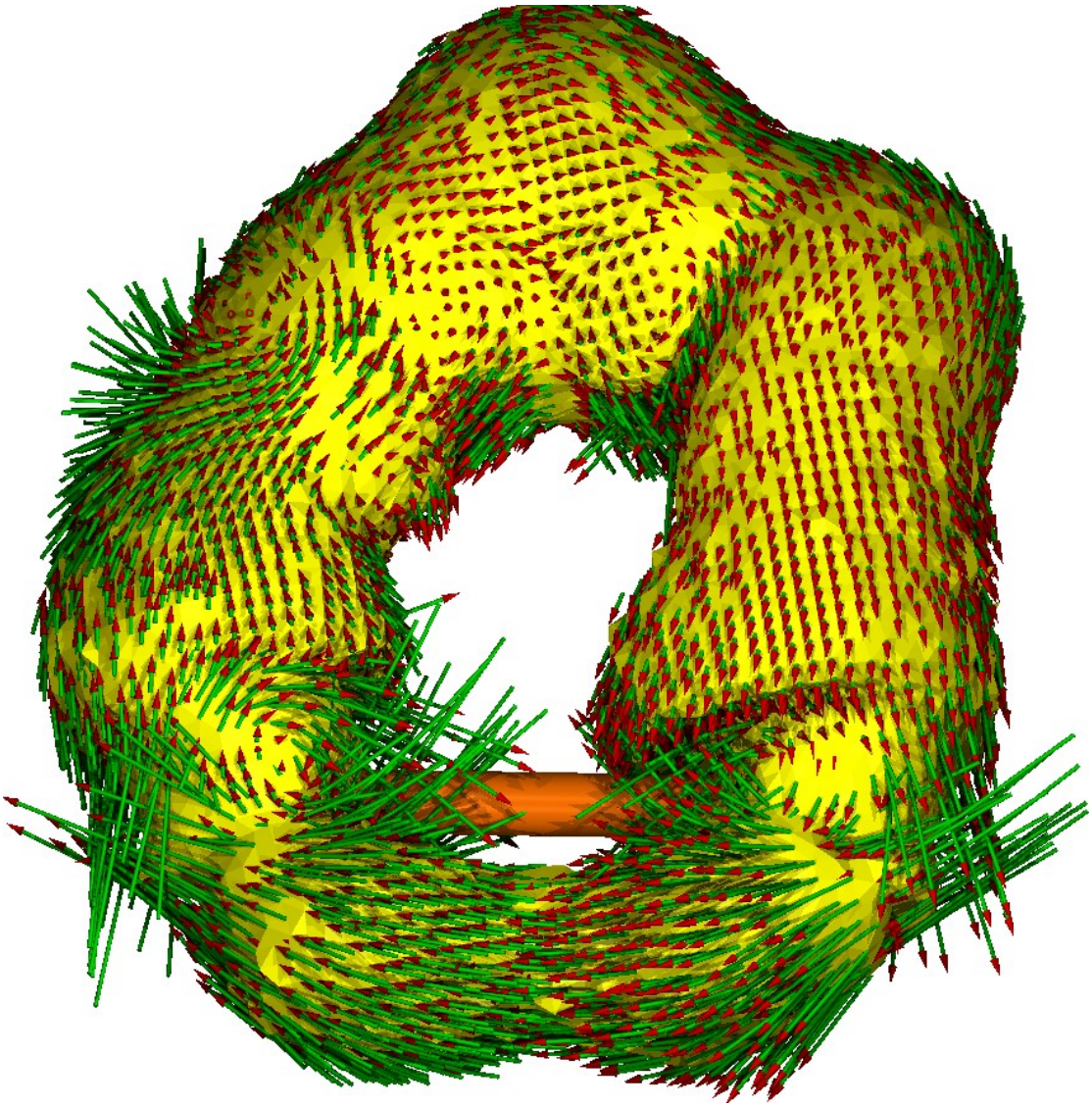

**Fig. S19** ACID isosurface (isovalue: 0.024 a.u.) of the $ON_2Bi_2$ ring in the $S_0$ state ($\sigma$).

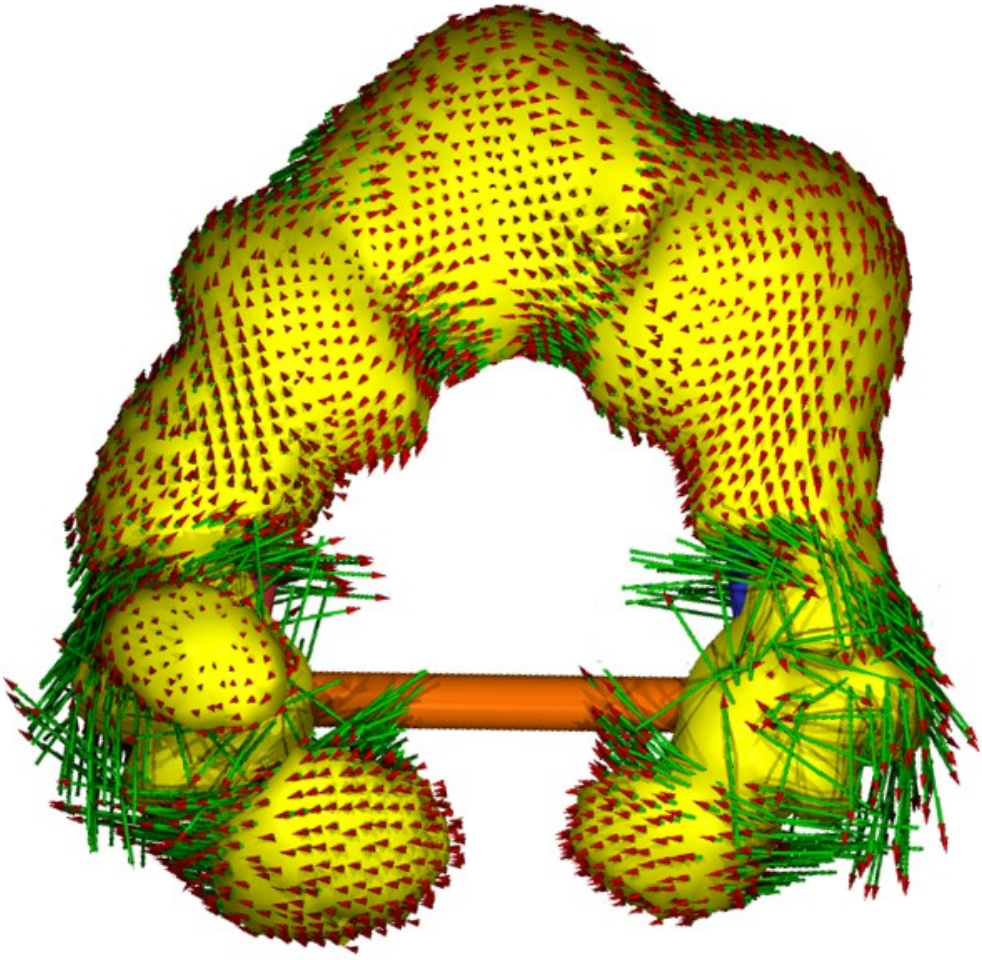

**Fig. S20** ACID isosurface (isovalue: 0.024 a.u.) of the $ON_2Bi_2$ ring in the $T_1$ state (total).

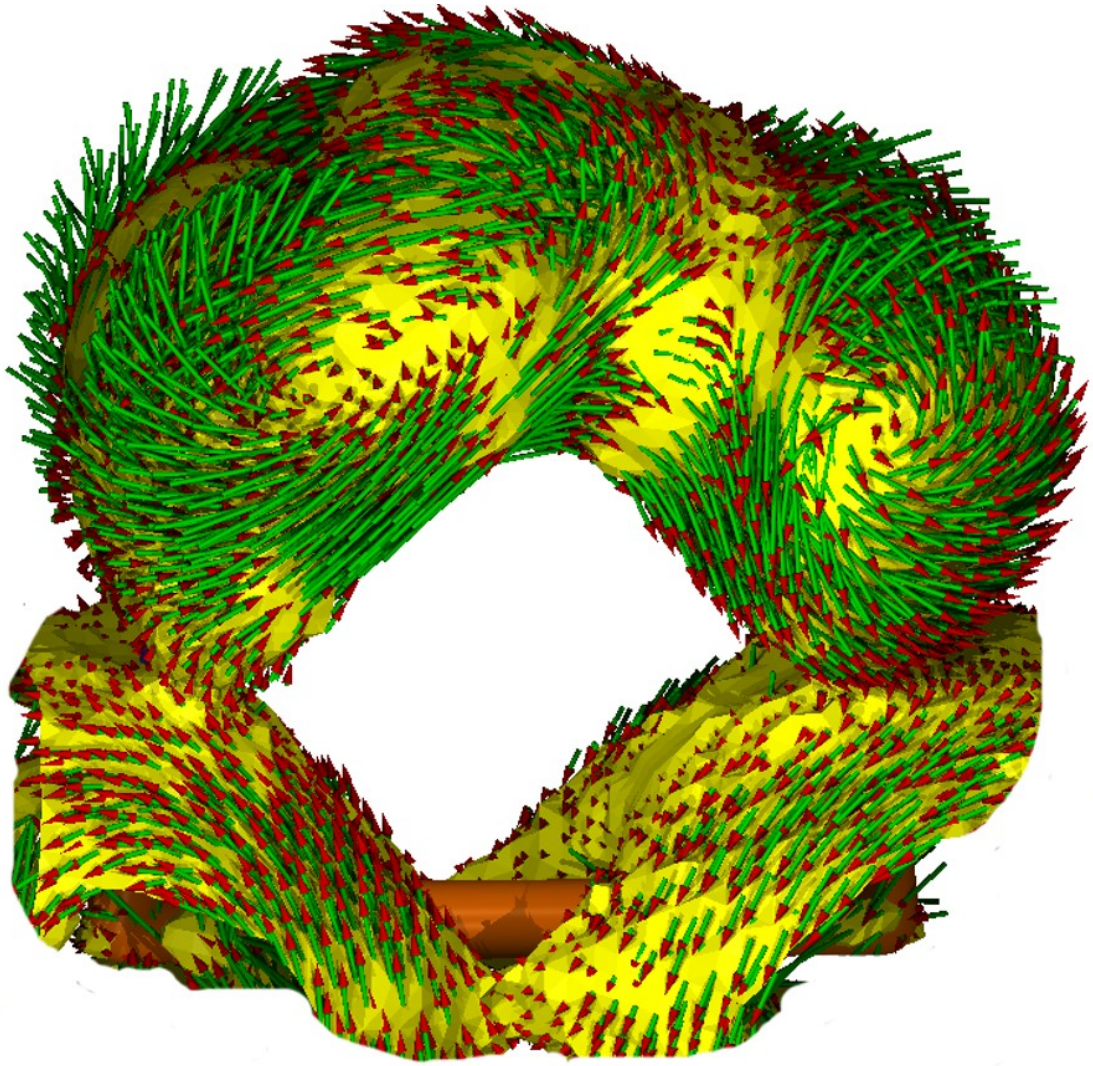

**Fig. S21** ACID isosurface (isovalue: 0.015 a.u.) of the $ON_2Bi_2$ ring in the $T_1$ state ($\pi$).

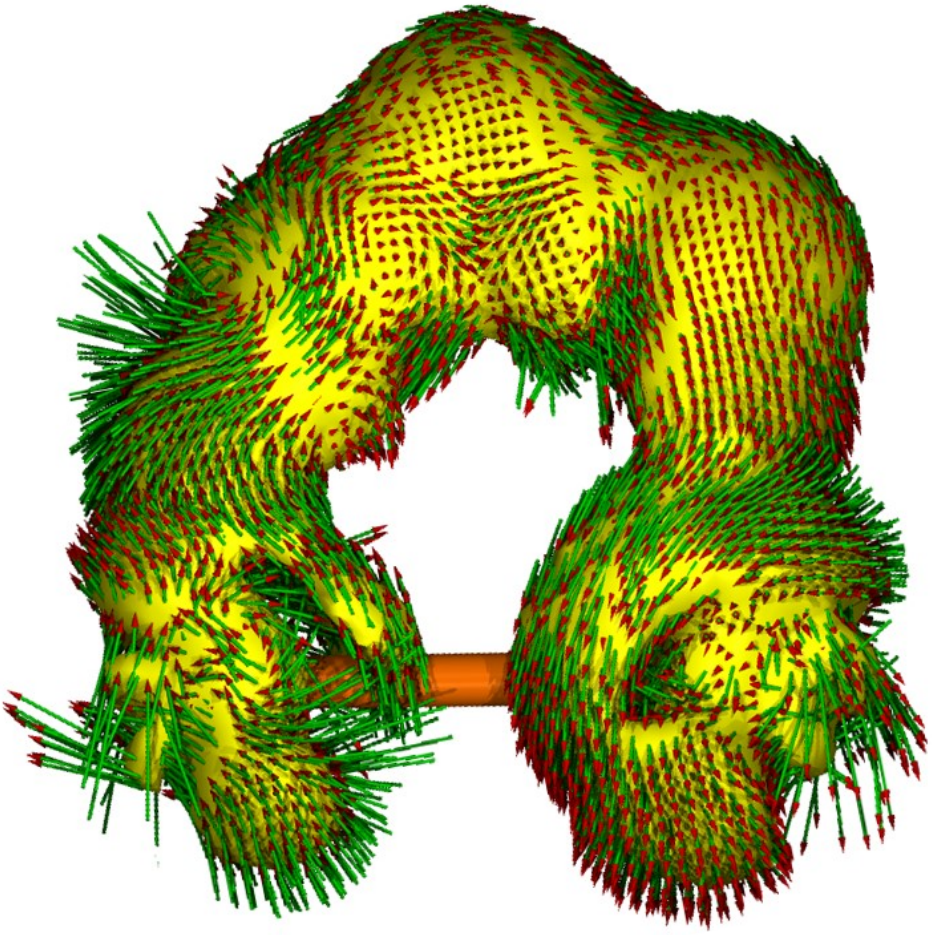

**Fig. S22** ACID isosurface (isovalue: 0.024 a.u.) of the $ON_2Bi_2$ ring in the $T_1$ state ($\sigma$).

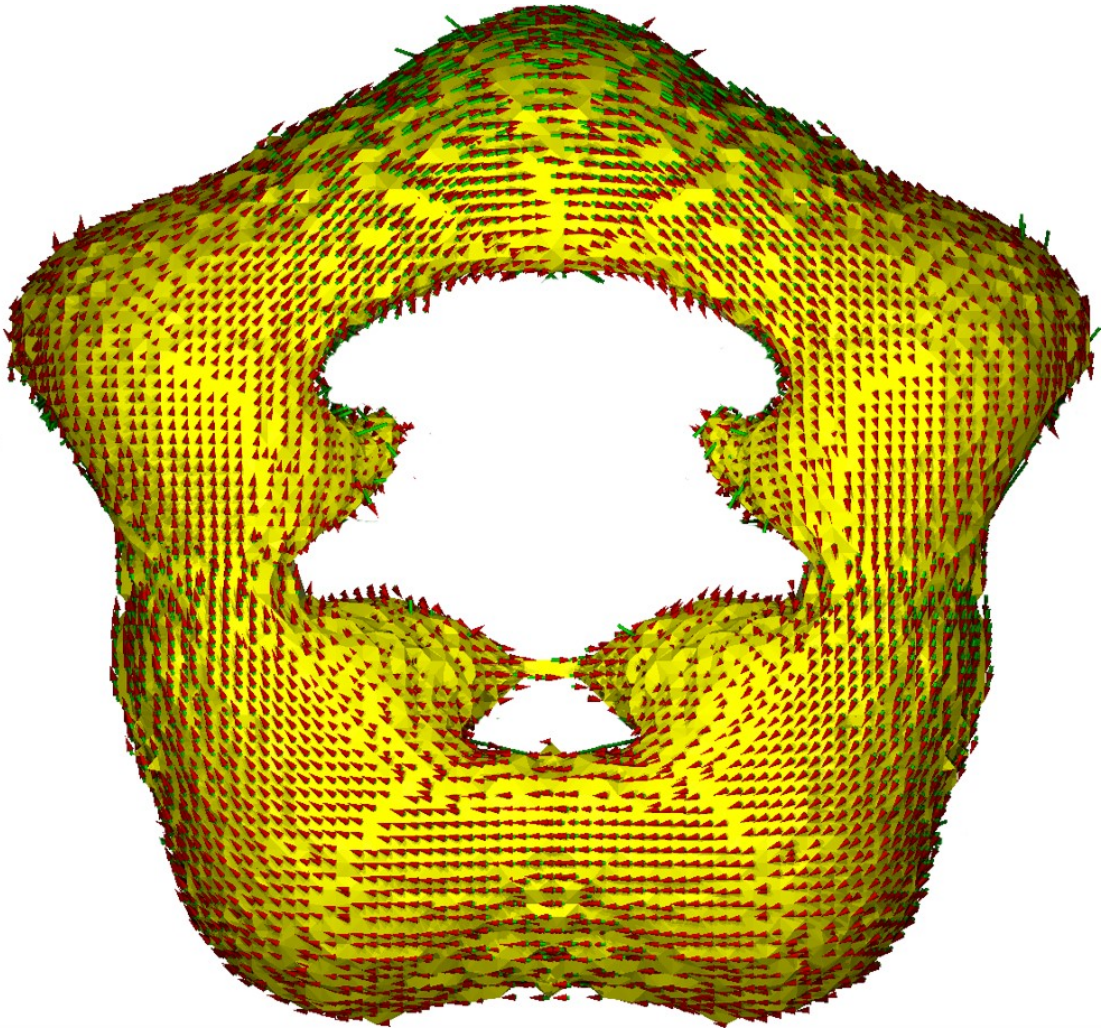

**Fig. S23** ACID isosurface (isovalue: 0.024 a.u.) of the $SAs_2Sb_2$ ring in the $S_0$ state (total).

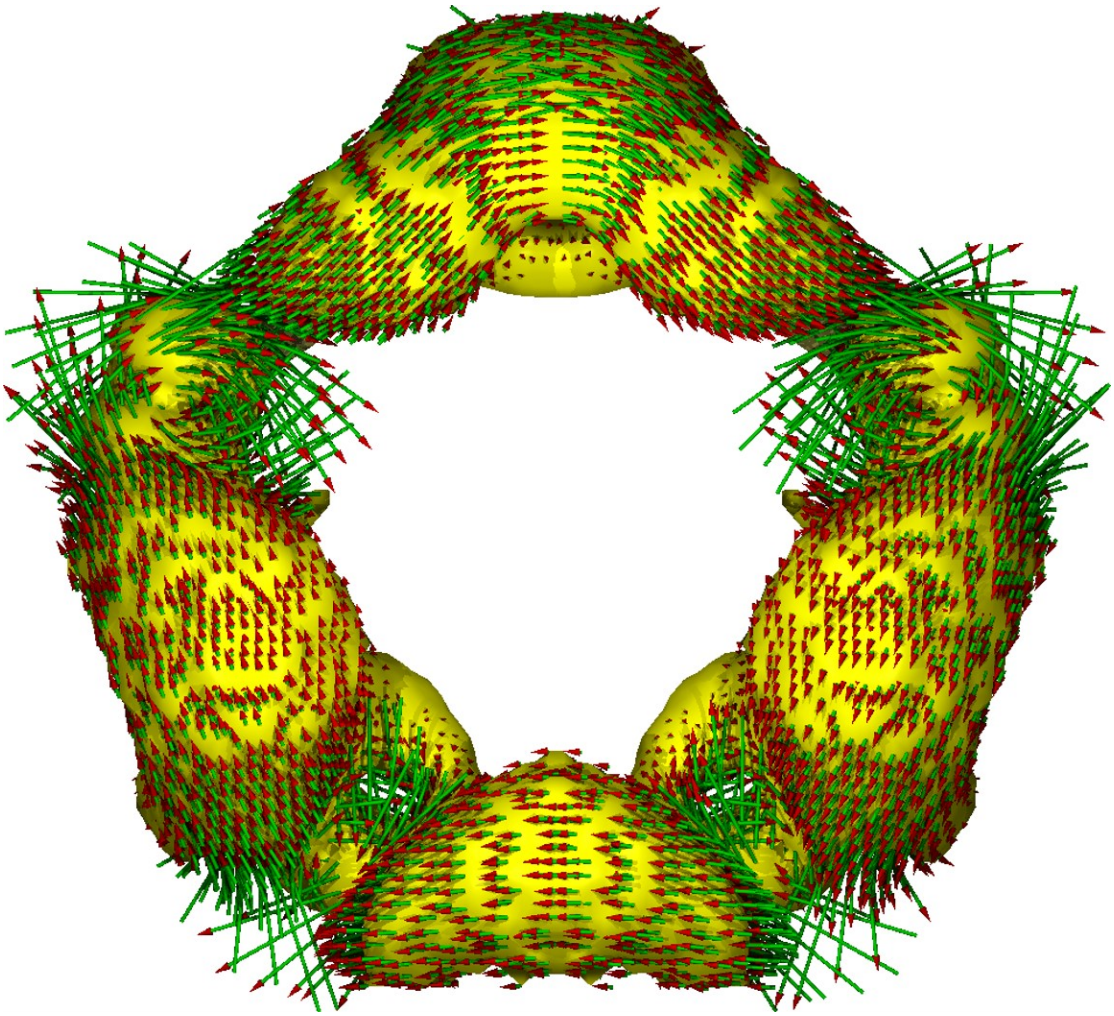

**Fig. S24** ACID isosurface (isovalue: 0.024 a.u.) of the $SAs_2Sb_2$ ring in the $S_0$ state ($\pi$).

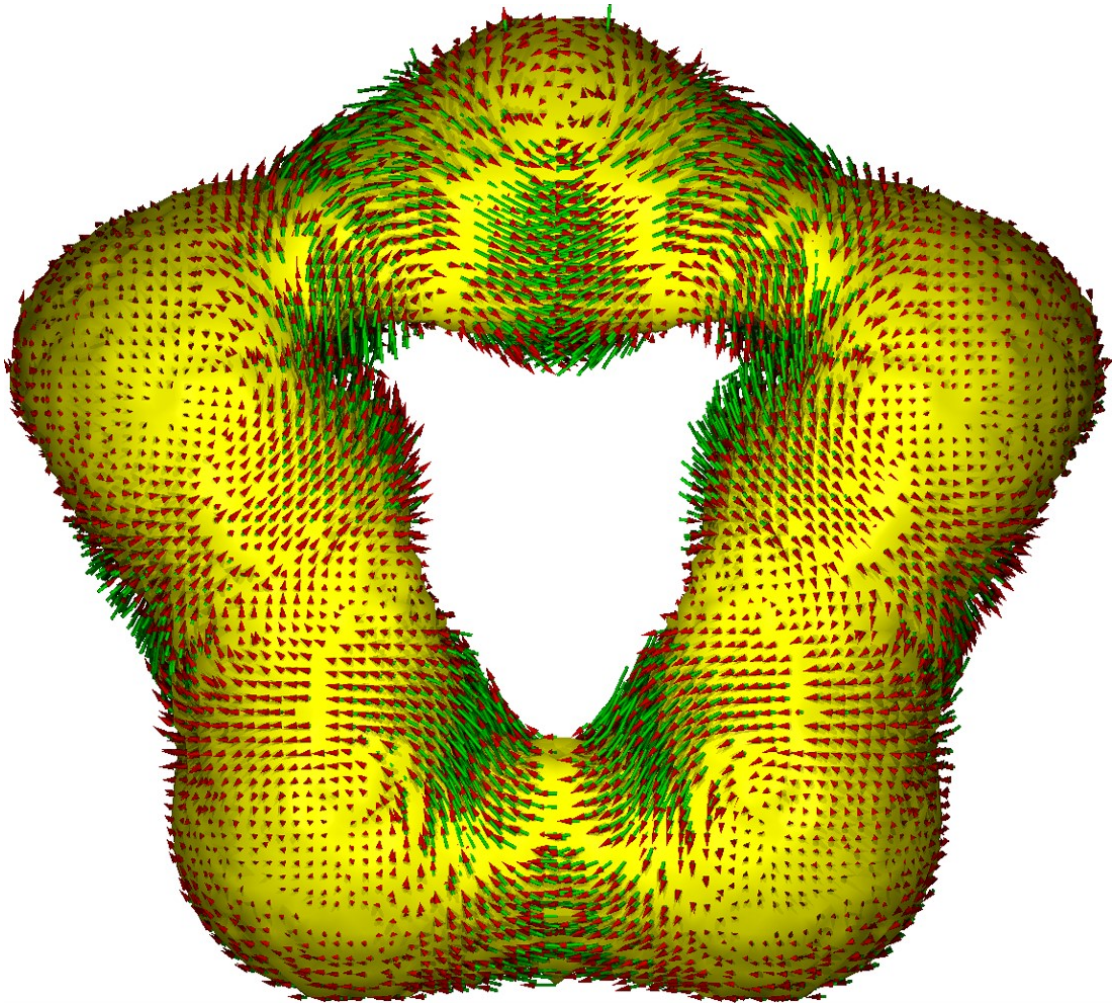

**Fig. S25** ACID isosurface (isovalue: 0.024 a.u.) of the $SAs_2Sb_2$ ring in the $S_0$ state ($\sigma$).

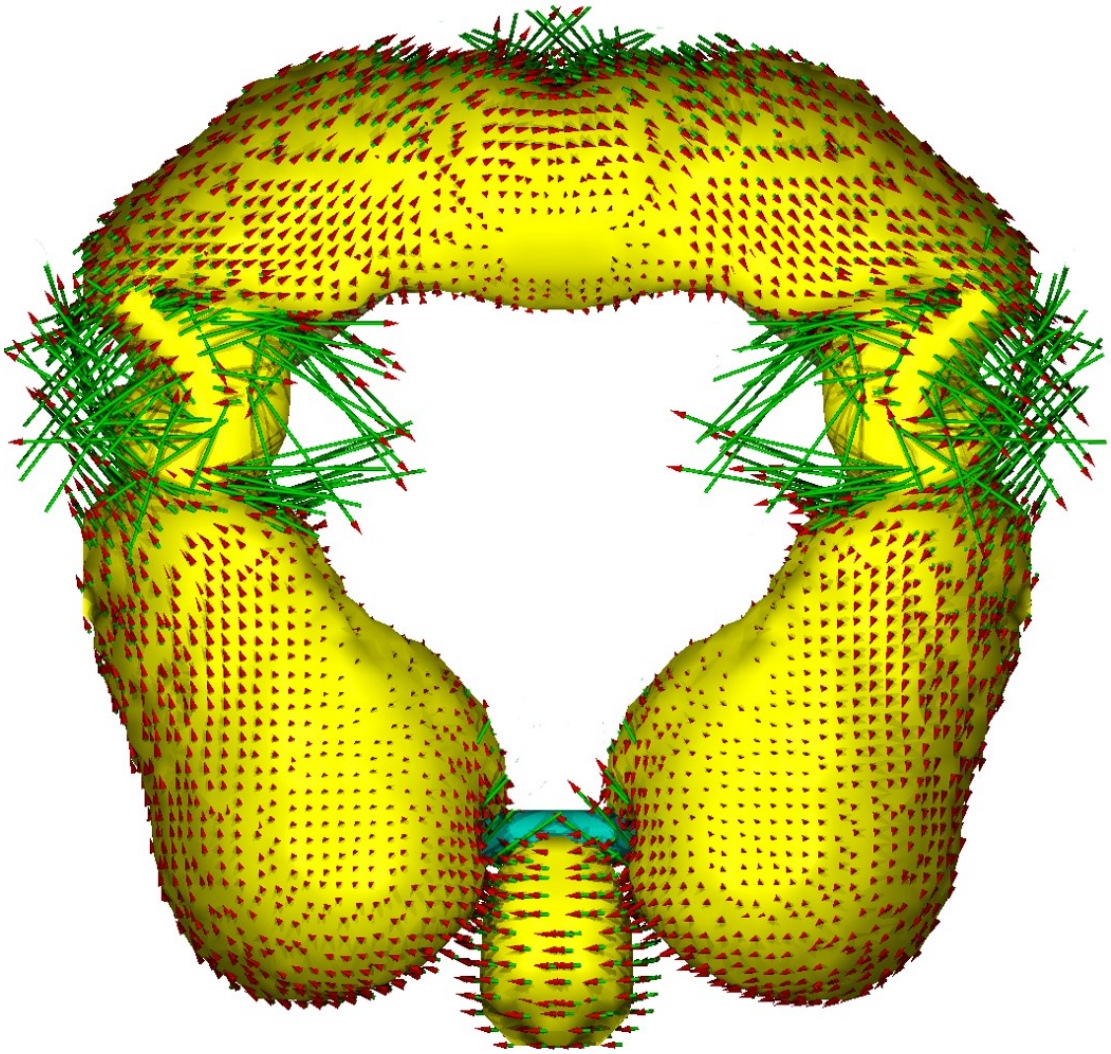

**Fig. S26** ACID isosurface (isovalue: 0.024 a.u.) of the $SAs_2Sb_2$ ring in the $T_1$ state (total).

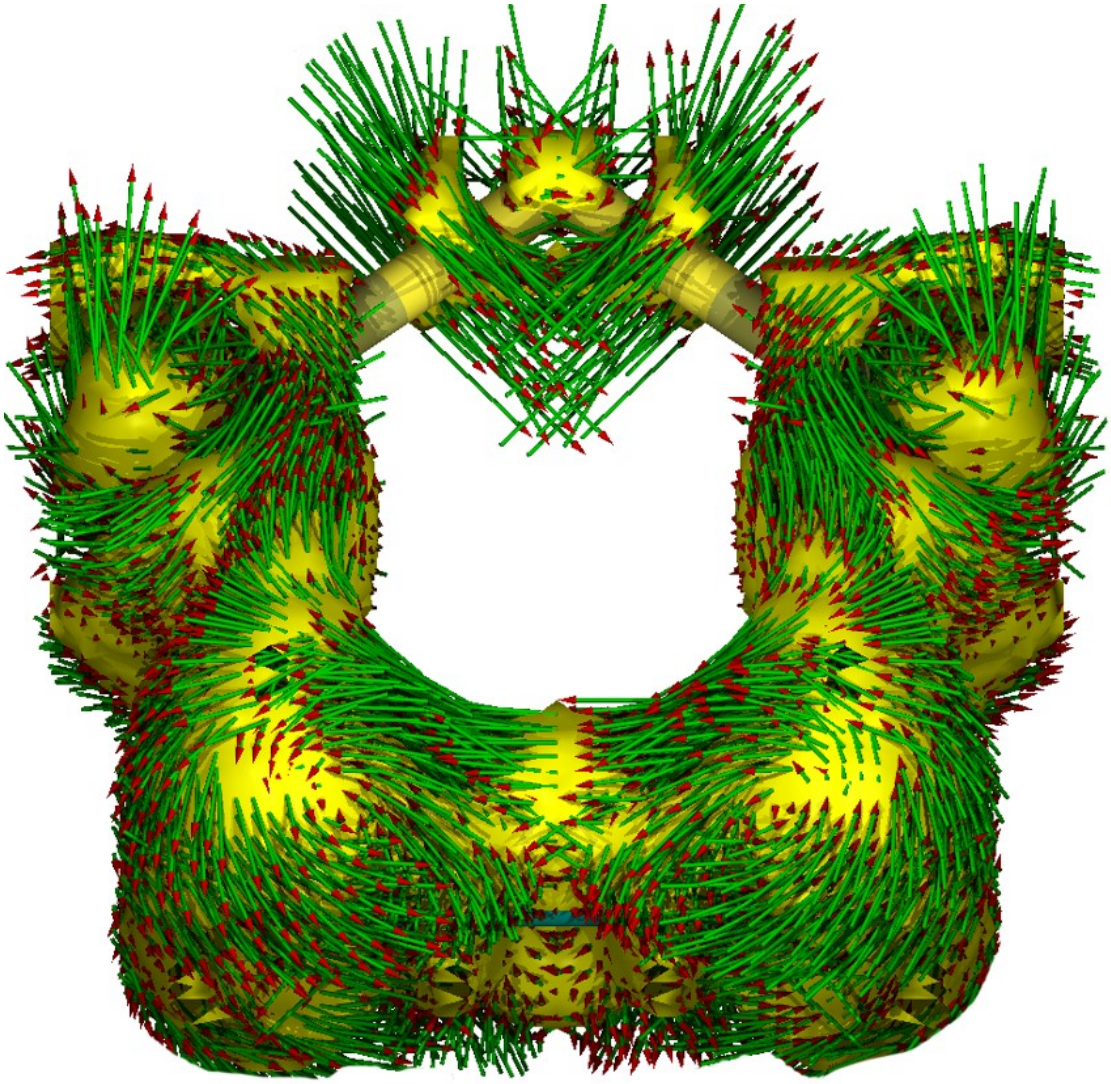

**Fig. S27** ACID isosurface (isovalue: 0.024 a.u.) of the $SAs_2Sb_2$ ring in the $T_1$ state ($\pi$).

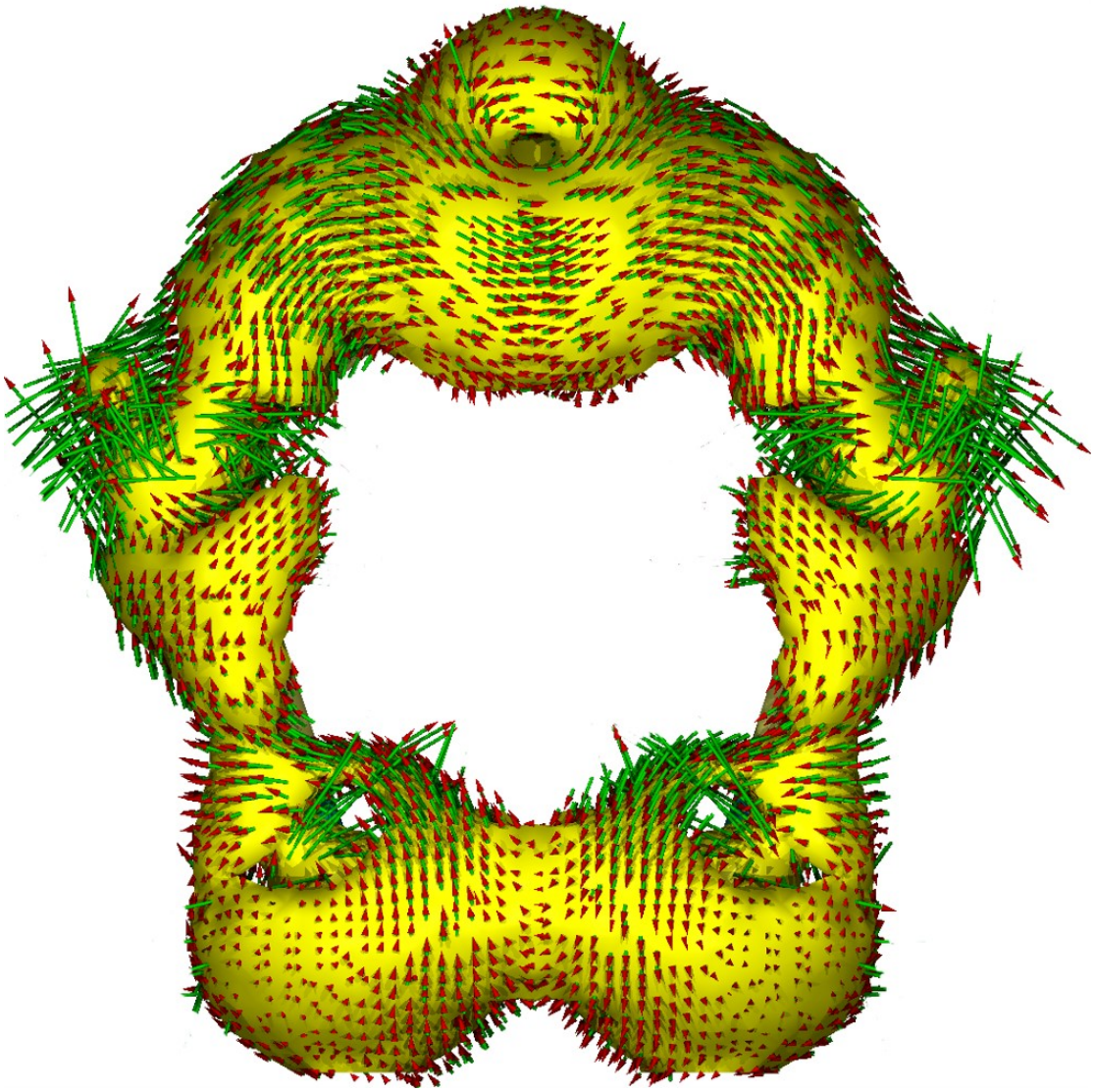

**Fig. S28** ACID isosurface (isovalue: 0.024 a.u.) of the $SAs_2Sb_2$ ring in the $T_1$ state ($\sigma$).

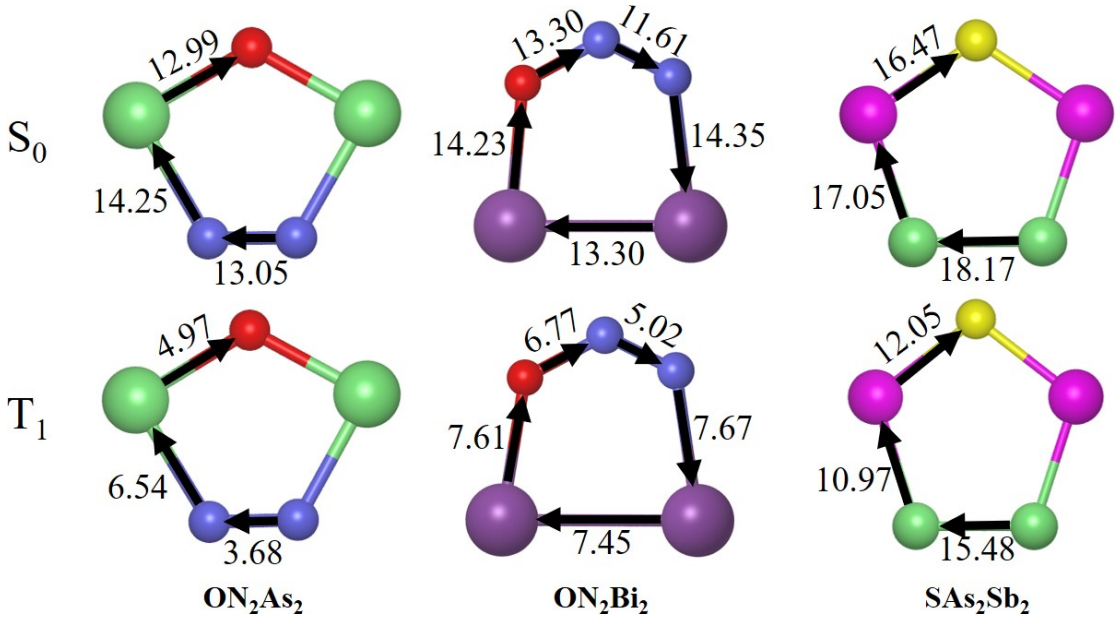


**Fig. S29** The strength of magnetically induced ring current (unit: nA $T^{-1}$) along selected bonds of $ON_2As_2$, $ON_2Bi_2$ and $SAs_2Sb_2$ in two electronic states. The slight differences in the ring-current strengths for the ring bonds are due to the tilted vortex which causes the integration does not begin in the vortex center for all z values.

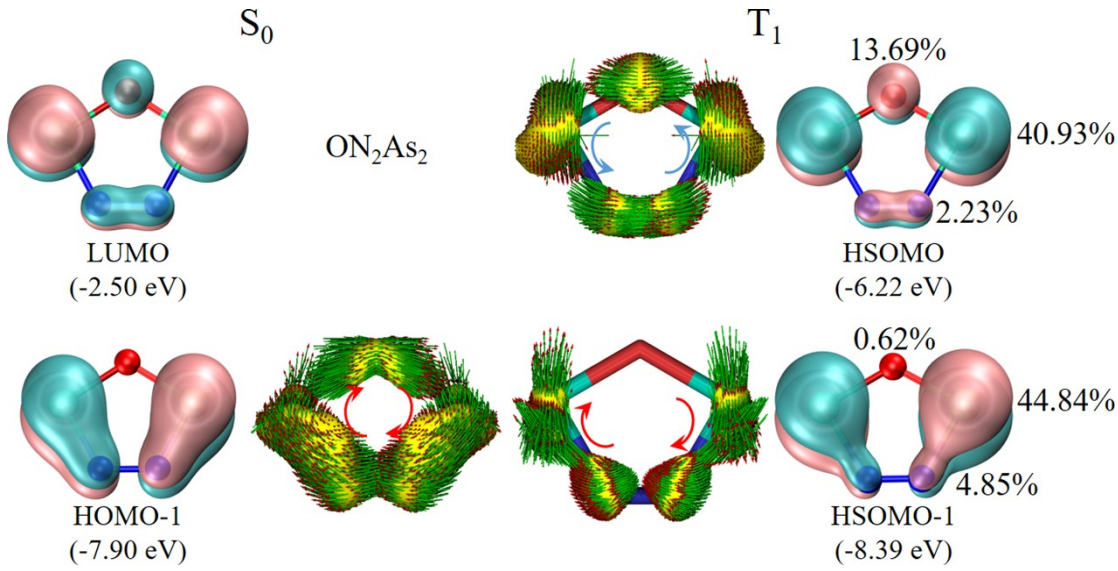


**Fig. S30** ACID isosurfaces (isovalue: 0.024 a.u.) for the frontier molecular orbitals involved in the electron excitation from the $S_0$ to $T_1$ state of $ON_2As_2$. The contribution (%) of each atom to the HSOMO/HSOMO-1 is given.

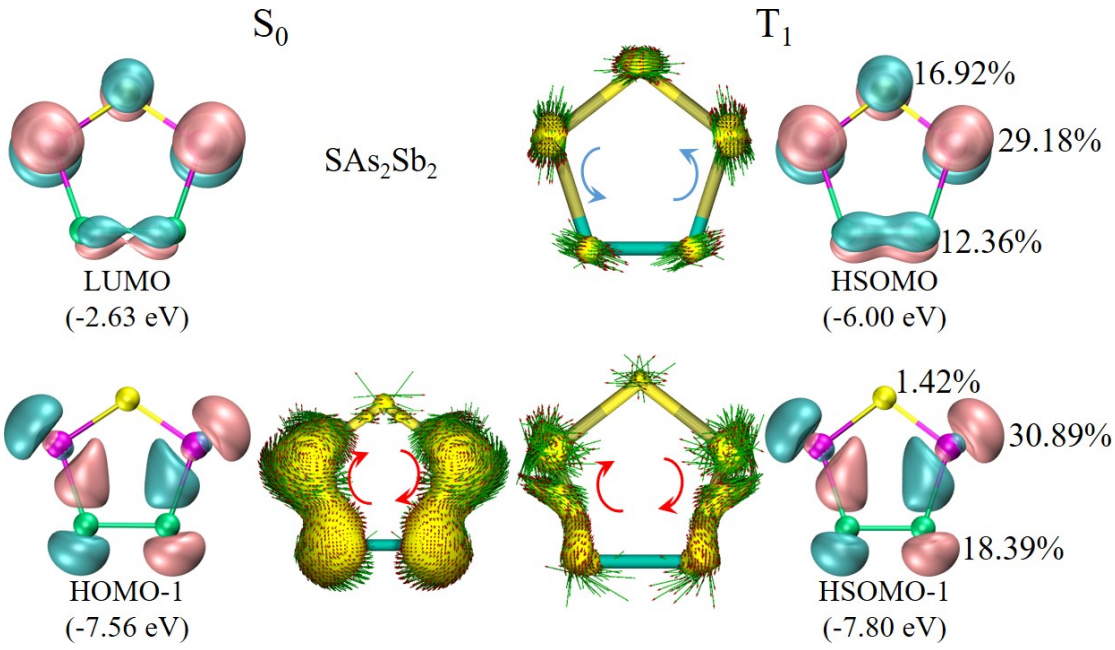


**Fig. S31** ACID isosurfaces (isovalue: 0.024 a.u.) for the molecular orbitals involved in the electron excitation from the $S_0$ to $T_1$ state of $SAs_2Sb_2$. The contribution (%) of each atom to the HSOMO/HSOMO-1 is given.

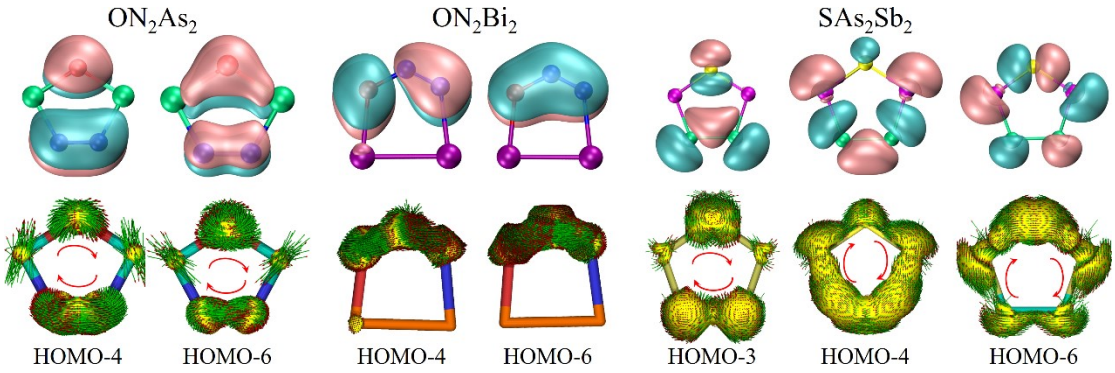


**Fig. S32** ACID isosurfaces (isovalue: 0.024 a.u.) for selected molecular orbitals of $ON_2As_2$, $ON_2Bi_2$ and $SAs_2Sb_2$ in the $S_0$ state.

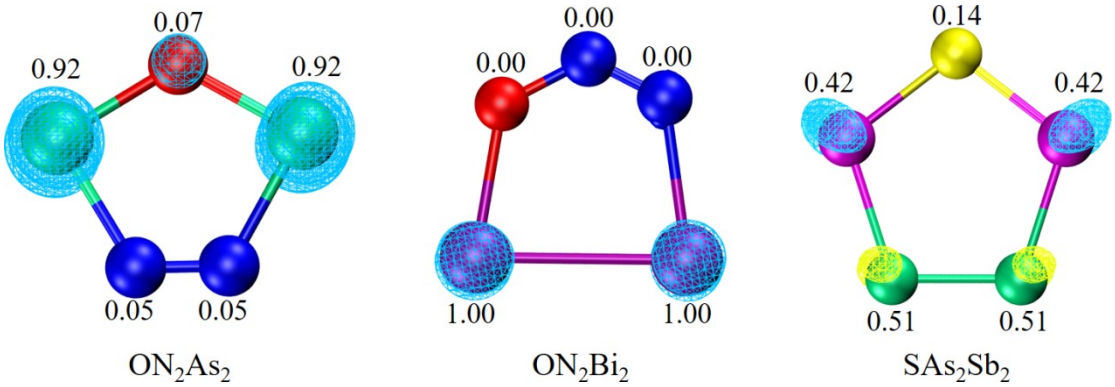


**Fig. S33** Spin density distributions (isovalue: 0.02 a.u.) with spin values for the $T_1$ state of $ON_2As_2$, $ON_2Bi_2$ and $SAs_2Sb_2$.

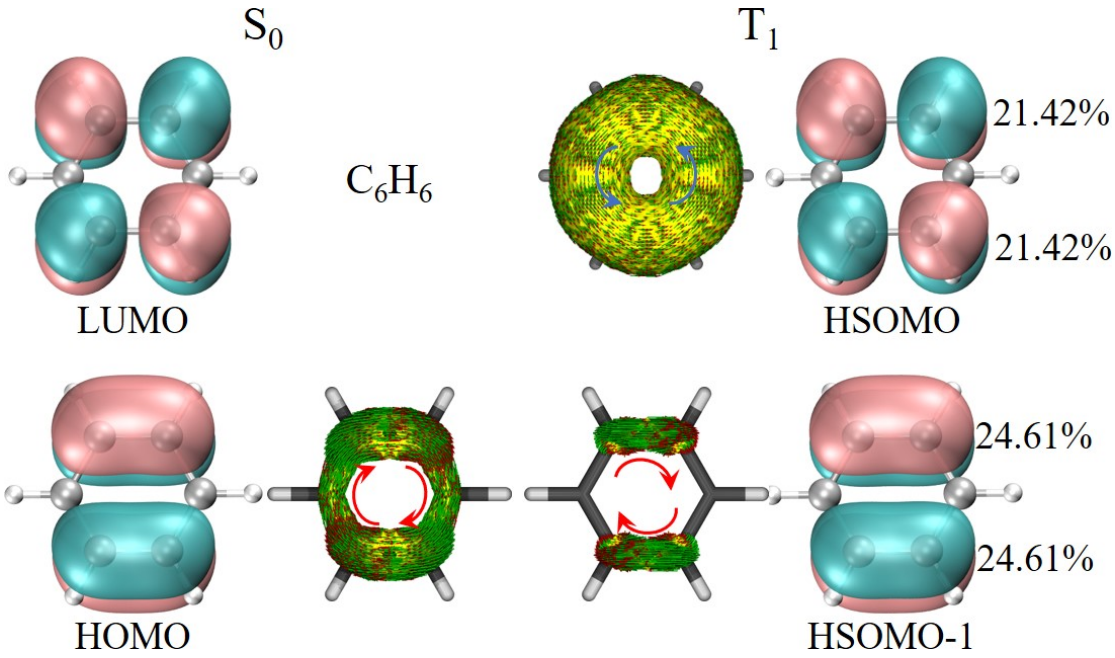


**Fig. S34** ACID isosurfaces (isovalue: 0.024 a.u.) for the molecular orbitals involved in the electron excitation from the $S_0$ to $T_1$ state of Bz. The contribution (%) of each atom to the HSOMO/HSOMO-1 is given.

**Optimized Cartesian coordinates**

**$ON_2As_2(S_0)$**

| | | | |
|---|---|---|---|
| O | 0.00000000 | 0.00000000 | 1.11992220 |
| As | 0.00000000 | 1.49394753 | 0.15991780 |
| As | 0.00000000 | -1.49394753 | 0.15991780 |
| N | 0.00000000 | 0.65657766 | -1.39385374 |
| N | 0.00000000 | -0.65657766 | -1.39385374 |

**$ON_2As_2(T_1)$**

| | | | |
|---|---|---|---|
| O | 0.00000000 | 0.00000000 | 1.07924614 |
| As | 0.00000000 | 1.55169894 | 0.18183321 |
| As | 0.00000000 | -1.55169894 | 0.18183321 |
| N | 0.00000000 | 0.59121408 | -1.47392579 |
| N | 0.00000000 | -0.59121408 | -1.47392579 |

**$ON_2Bi_2(S_0)$**

| | | | |
|---|---|---|---|
| O | 2.04879830 | -0.74665247 | 0.00000000 |
| N | 2.43910899 | 0.53858803 | 0.00000000 |
| N | 1.68409795 | 1.47265005 | 0.00000000 |
| Bi | 0.00000000 | -1.37320402 | 0.00000000 |
| Bi | -0.54521488 | 1.27554804 | 0.00000000 |

**$ON_2Bi_2(T_1)$**

| | | | |
|---|---|---|---|
| O | 2.03451215 | 0.76289405 | 0.00000000 |
| N | 2.44129518 | -0.53395604 | 0.00000000 |
| N | 1.71936712 | -1.48449811 | 0.00000000 |
| Bi | 0.00000000 | 1.49447811 | 0.00000000 |
| Bi | -0.54699704 | -1.39777810 | 0.00000000 |

**$SAs_2Sb_2(S_0)$**

| | | | |
|---|---|---|---|
| S | 0.00000000 | 0.00000000 | 2.05152039 |
| Sb | 0.00000000 | 1.97133122 | 0.71563373 |
| Sb | 0.00000000 | -1.97133122 | 0.71563373 |
| As | 0.00000000 | -1.17601339 | -1.60331769 |
| As | 0.00000000 | 1.17601339 | -1.60331769 |

**$SAs_2Sb_2(T_1)$**

| | | | |
|---|---|---|---|
| S | -0.00003818 | -0.00000002 | 2.22252397 |
| Sb | 0.00003080 | 1.91336006 | 0.74045750 |
| Sb | 0.00003080 | -1.91336014 | 0.74045756 |
| As | -0.00001171 | -1.12656825 | -1.71364243 |
| As | -0.00001171 | 1.12656836 | -1.71364258 |

## Notes and references

S1 T. Lu, *J. Mol. Model.*, 2021, **27**, 263.